High-order quantum back-reaction and quantum cosmology with a positive cosmological constant

Martin Bojowald,[1] David Brizuela,[1] Hector H. Hernández,[2] Michael J. Koop,[1] and Hugo A. Morales-Técotl[3]

[1]*Institute for Gravitation and the Cosmos, The Pennsylvania State University,
104 Davey Lab, University Park, Pennsylvania 16802, USA*
[2]*Universidad Autónoma de Chihuahua, Facultad de Ingeniería, Nuevo Campus Universitario, Chihuahua 31125, México*
[3]*Departamento de Física, Universidad Autónoma Metropolitana Iztapalapa, San Rafael Atlixco 186, CP 09340, México D.F., México*

When quantum back-reaction by fluctuations, correlations and higher moments of a state becomes strong, semiclassical quantum mechanics resembles a dynamical system with a high-dimensional phase space. Here, systematic computational methods to derive the dynamical equations including all quantum corrections to high order in the moments are introduced, together with a (deparameterized) quantum cosmological example to illustrate some implications. The results show, for instance, that the Gaussian form of an initial state is maintained only briefly, but that the evolving state settles down to a new characteristic shape afterwards. Remarkably, even in the regime of large high-order moments, we observe a strong convergence within all considered orders that supports the use of this effective approach.

I. INTRODUCTION

Semiclassical approximations are of importance throughout physics in order to extract new effects or potentially observable phenomena in regimes in which quantum features are relevant but not dominant. All aspects of quantum gravity currently considered for potential tests fall in this class of situations. While deep quantum phases are crucial for several conceptual problems, the current developments remain so diverse that reliable conclusions are difficult to draw. Semiclassical physics, on the other hand, is already useful for this class of theories in order to demonstrate their consistency with large-scale properties of the universe and to approach potential low-energy observations for instance via details of the cosmic microwave background. For this reason, the development of systematic semiclassical approximations is one of the major requirements in current quantum-gravity research, especially for approaches such as loop quantum gravity whose underlying principles do not make use of a continuum geometry and perturbations around it.

In loop quantum gravity and cosmology, the main tool available at a dynamical level is that of effective equations which describe the evolution of expectation values in a dynamical state [1]. As in most quantum systems, especially interacting ones, quantum fluctuations, correlations and higher moments of the state then back-react on the evolution of expectation values, described in effective equations by coupling terms between classical and quantum degrees of freedom. With an infinite number of independent moments of a state, there are infinitely many quantum degrees of freedom, making the general system of equations difficult to analyze. In semiclassical regimes, however, the infinite set of equations reduces to finite sets at any given order of the expansion by powers of $\hbar$. In this

way, a systematic expansion arises that goes well beyond other examples such as the WKB approximation. To first order in $\hbar$ and combined with a second-order adiabatic approximation, applied to anharmonic oscillators, equations equivalent to those of the low-energy effective action are produced when expanding around the ground state [1,2]. (The more widely applied WKB approximation does not reproduce the low-energy effective action [3].) For other systems and different states, on the other hand, the canonical methods developed in [1] are more general and apply to quantum cosmology as well, even taking into account the totally constrained nature of these systems [4]. One should thus expect that an application to quantum gravity allows comparisons with low-energy effective quantum gravity [5,6], but can also highlight new effects related to specific properties of quantum space-time structure as opposed to just graviton dynamics on a classical background.

Compared with direct solution procedures of the partial differential equations that determine the dynamics of wave functions, the procedure used here has the advantage of directly yielding expressions for expectation values and other, in principle observable quantities. The usual, but often numerically cost-intensive two-step procedure of first finding expressions for the wave function and then performing integrations to obtain expectation values is thus significantly reduced. In this context, the methods used and described are useful not just for quantum cosmology, the realm of our examples, but may find wider applicability. In quantum cosmology, or more generally constrained systems, other advantages include a possible extension to systems in which the dynamics is determined by a Hamiltonian constraint, not a Hamiltonian function [4,7,8], and a simplification of the problem of time in semiclassical regimes [9,10].

The semiclassical approximation allows one to consider most cases of interest in current quantum-gravity research, but they do not allow one to tackle all of them. For this reason it is of interest to analyze the system of equations obtained as more and more of the moments grow large and become relevant when a dynamical state turns more highly quantum. Since such large numbers of variables coupled to each other by long evolution equations are difficult to handle analytically (see the Appendix for deterrence), the main aim of this article is to provide results of efficient computer-algebra codes designed to derive these equations automatically and quickly to high orders, which can then be fed into a numerical solver of the coupled differential equations. In this way, one can see how much high orders of the expansions matter and how higher moments can affect the evolution of expectation values as strong quantum regimes are approached.

An interesting toy example for this is a spatially flat isotropic universe with a positive cosmological constant, filled with a homogeneous free and massless scalar field. The free scalar can play the role of a global internal time, allowing one to reformulate the constrained system as ordinary Hamiltonian evolution. In the presence of a positive cosmological constant, the value of the scalar field
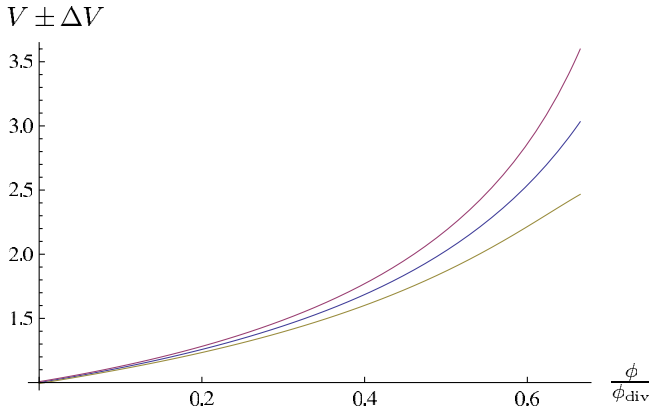

FIG. 1 (color online). In this plot we show the evolution of the volume expectation value V for a cosmological constant $\Lambda = 9 \times 10^7$ and initial data to be presented in Sec. IV E, together with the spread around this trajectory $V \pm \Delta V$. This plot illustrates the growing dispersion of a state evolving to large volume. The range for ϕ shown, relative to the value ϕ_{div} at which the classical volume diverges, is the maximal one obtained with numerical stability to tenth order of moments of the evolving state. As the volume grows, the area swept out by the wave packet more and more aligns itself with the vertical axis, such that volume fluctuations (as well as some other moments) computed at a fixed value of ϕ diverge. This divergence would happen even if the state remained sharply peaked transversal to the direction in which it moves, and is thus not a failure of semiclassicality in this system but rather an artifact of the parametrization of evolution. Physical implications are thus difficult to draw, but an interesting test case for back-reaction issues is obtained.

is bounded from above as a function of time; thus, when using the scalar as internal time, infinite volume is reached at a finite time ϕ_{div}. As this point is approached, volume fluctuations and higher moments diverge even though the regime is supposed to be one of low-curvature nature (see Fig. 1). The nonsemiclassical appearance is an artifact of the choice of time, highlighting the toy-nature of the model. Physical conclusions derived from the model for a late-time universe with a positive cosmological constant can thus not be reliable, as interesting as they might be. But the model is ideal for a mathematical analysis of the possible roles of large moments. In the present article, we will use this example mainly to illustrate the usefulness of the numerical codes; further analysis requires more sophisticated methods to handle the large parameter space of all moments.

II. GENERAL FORMALISM

We begin with a brief review of the procedure of effective equations, followed by a correction of an important formula of [1] and its accompanying proof.

A. Quantum state space

Classically, the phase space of a system with one degree of freedom is completely described by the generalized position V (related to the volume in cosmological models) and its conjugate momentum P (related to the Hubble parameter). During the quantization process each classical phase-space function is promoted to an operator, and observable information is extracted via expectation values which can be seen as functionals on the algebra of operators that characterize states. Since expectation values of products of operators in general differ from products of expectation values, the following infinitely many moments are needed to describe the system completely:

$$G^{a,b} := \langle (\hat{P} - P)^a (\hat{V} - V)^b \rangle_{\mathrm{Weyl}}, \qquad (1)$$

where the subscript Weyl stands for totally symmetric ordering. Moments cannot be chosen arbitrarily but are subject to additional conditions such as the uncertainty relation

$$G^{2,0} G^{0,2} - (G^{1,1})^2 \geq \frac{\hbar^2}{4}. \qquad (2)$$

Moreover, a set of moments satisfying all those conditions in general corresponds to a mixed rather than pure state. By considering moments to describe states, mixing (which is important for generic descriptions of homogeneous quantum cosmology seen as an averaged description of microscopic physics, in particular, inhomogeneities) is automatically included.

The use of moments allows a very general definition of semiclassical states as those satisfying the hierarchy $G^{a,b} = O(\hbar^{(a+b)/2})$, realized for Gaussian states (see

below) but also for a much wider class. This characterization of semiclassical states (pure or mixed) has two major advantages: (i) It is a general characterization, as unbiased as possible. (In more restrictive classes such as Gaussians the specific form of the wave function may actually matter for physical effects.) (ii) The infinitely many $G^{a,b}$ are decomposed in finite sets to order $\hbar^n$. This feature allows systematic approximations of semiclassical dynamics.

The moments are pure quantum degrees of freedom; they would all vanish in a classical limit. In a quantized interacting system they couple to the expectation values $P := \langle \hat{P} \rangle$ and $V := \langle \hat{V} \rangle$. The state with respect to which these moments are taken is specified via values for all the quantum variables, which are all dynamical and satisfy equations of motion. In order to consider the evolution of expectation values, the evolution of all moments must be followed simultaneously. Assuming the moments to be constant or to take specific values such as, for instance, those of a Gaussian state at all times cannot provide the correct dynamics. The dynamics is described by a quantum Hamiltonian, the expectation value of the Hamiltonian operator, which is state dependent and thus a function of expectation values and all the moments. By Taylor expansion, one can write the quantum Hamiltonian as

$$H_Q(V, P, G^{a,b}) = \langle \hat{H} \rangle = H + \sum_{a=0}^{\infty} \sum_{b=0}^{\infty} \frac{1}{a! b!} \frac{\partial^{a+b} H}{\partial P^a \partial V^b} G^{a,b},$$

(3)

with the classical Hamiltonian H. The quantum variables it contains provide crucial corrections to the classical dynamics in a state-dependent way. We note that expansions of this form (as also the Feynman or WKB expansions) are expected to be asymptotic, not necessarily convergent. In the model discussed below, we will nevertheless observe strong convergence properties within a large range of orders.

The evolution generated by the quantum Hamiltonian H_Q, governed by the equations of motion $df/d\phi = \{f, H_Q\}$ for phase-space functions f, is described with respect to a time parameter ϕ. This could be an absolute time parameter or, as in the example used below, an internal time variable chosen for a deparameterizable constrained system. (For the effective treatment of nondeparameterizable constrained systems, lacking a global internal time, see [9,10].) Effective quantum evolution then provides an approximation scheme for time-dependent expectation values of operators, starting with some initial state specified by the initial expectation values and moments. It is straightforward to find moments corresponding to a wave-function representation of the initial state in a Hilbert space, such as the Schrödinger one. Moments evolved by the quantum Hamiltonian then correspond to the dynamical state, evolved in the Schrödinger or Heisenberg picture. We are thus guaranteed that at all times, as long as the evolved moments remain finite, there

is still a corresponding wave function with those moments to within the order of approximation considered. It may be difficult to construct such a wave function explicitly, but this is not required because the information relevant for observations is already contained in the expectation values and moments. (When moments diverge, as in the example discussed below, the state moves out of the domain of definition of the operators considered. By our moment expansions we will only consider the approach to such a point of divergence, not the point itself.)

In order to obtain all Hamiltonian equations of motion in the context of this effective approach, we will need to compute the Poisson brackets between any two moments. If one defines the Poisson bracket for expectation values of arbitrary operators $\hat{X}$ and $\hat{Y}$ by the relation $\{\langle \hat{X} \rangle, \langle \hat{Y} \rangle\} = -i\hbar^{-1} \langle [\hat{X}, \hat{Y}] \rangle$ (extended to arbitrary functions of expectation values using linearity and the Leibniz rule), Hamiltonian equations of motion generated by $H_Q = \langle \hat{H} \rangle$ are equivalent to the Schrödinger flow of states or the Heisenberg flow of operators. By applying this relationship to all powers of the basic operators, the Poisson brackets between moments is obtained. Since $[\hat{V}, \hat{P}] = i\hbar$, in the particular case of the basic operators themselves, the Poisson bracket reduces to the classical one, $\{V, P\} = 1$. Moreover, one can easily show that moments have vanishing Poisson brackets with the basic expectation values:

$$\{G^{a,b}, V\} = 0 = \{G^{a,b}, P\}.$$

(4)

The general case of Poisson brackets between moments is more involved. We have the general formula

$$\{G^{a,b}, G^{c,d}\} = ad G^{a-1,b} G^{c,d-1} - bc G^{a,b-1} G^{c-1,d}$$
$$+ \sum_n \left(\frac{i\hbar}{2} \right)^{n-1} K_{abcd}^n G^{a+c-n,b+d-n},$$

(5)

where the sum over n runs over all odd numbers from 1 to $\text{Min}(a + c, b + d, a + b, c + d)$, which makes the coefficients real in spite of the presence of the imaginary unit. We have also defined

$$K_{abcd}^n := \sum_{m=0}^{n} (-1)^m m! (n-m)! \binom{a}{m} \binom{b}{n-m}$$
$$\times \binom{c}{n-m} \binom{d}{m}$$
$$= 2^n \sum_{m=0}^{n} (-1)^m C_{ad}^m C_{bc}^{n-m},$$

(6)

where the C-coefficients come from the Weyl ordering (see also Sec. III) and are defined as

$$C_{kn}^d := \frac{n! k!}{(n-d)! (k-d)! (2d)!!} = \frac{d!}{2^d} \binom{n}{d} \binom{k}{d}.$$

(7)

Note that these coefficients have the permutation property $K^n_{abcd} = (-1)^n K^n_{cdab}$. Since the sum in (5) is only over odd n, this makes the antisymmetry of the Poisson brackets transparent. (In these formulas, $G^{0,0} = 1$, $G^{0,1} = G^{1,0} = 0$, and $G^{a,b} = 0$ for any a or $b < 0$ are understood.)

A general formula analogous to (5) was obtained in [1], but since it was not applied to moments of high orders, a typo remained undiscovered. This typo is corrected in (5), and since the formula plays an important role for the results of this article, we provide a detailed proof in the following subsection.

B. Poisson structure of moments

As in [1], we consider the generating function,

$$D(\alpha) = \langle e^{\alpha_P(\hat{P}-P)+\alpha_V(\hat{V}-V)} \rangle$$

$$= \sum_{j=0}^{\infty} \sum_{k=0}^{j} \frac{1}{j!} \binom{j}{k} \langle \alpha_P^{j-k} \alpha_V^k [(\hat{P}-P)^{j-k}(\hat{V}-V)^k]_{\text{Weyl}} \rangle$$

$$= \sum_{j=0}^{\infty} \sum_{k=0}^{j} \frac{1}{k!(j-k)!} \alpha_P^{j-k} \alpha_V^k G^{j-k,k}. \qquad (8)$$

Assuming that the wave function is analytic in the mean values, $D(\alpha)$ and the Poisson bracket between two of these functions will also be analytic, which allows us to take the Taylor expansion to all orders in α,

$$\{D(\alpha), D(\beta)\} = \sum_{w=0}^{\infty} \sum_{x=0}^{w} \sum_{y=0}^{\infty} \sum_{z=0}^{y} \frac{\alpha_P^{w-x} \alpha_V^x \beta_P^{y-z} \beta_V^z}{x!(w-x)!z!(y-z)!}$$

$$\times \{G^{w-x,w}, G^{y-z,y}\}. \qquad (9)$$

On the other hand, we use the Baker-Campbell-Hausdorff formula to get the commutator

$$[e^{\alpha_P\hat{P}+\alpha_V\hat{V}}, e^{\beta_P\hat{P}+\beta_V\hat{V}}] = 2i \sin\left(\frac{\hbar}{2}(\alpha_V\beta_P - \alpha_P\beta_V)\right)$$

$$\times e^{(\alpha_P+\beta_P)\hat{P}+(\alpha_V+\beta_V)\hat{V}}, \qquad (10)$$

which gives us the Poisson bracket

$$\{D(\alpha), D(\beta)\} = \frac{2}{\hbar} \sin\left(\frac{\hbar}{2}(\alpha_V\beta_P - \alpha_P\beta_V)\right)D(\alpha+\beta)$$

$$- (\alpha_V\beta_P - \alpha_P\beta_V)D(\alpha)D(\beta). \qquad (11)$$

We then use a Taylor series and the binomial theorem to expand the right-hand side of the last equation. For the first term we get the expression,

$$\frac{2}{\hbar} \sin\left(\frac{\hbar}{2}(\alpha_V\beta_P - \alpha_P\beta_V)\right)D(\alpha+\beta)$$

$$= \frac{2}{\hbar}\left[\sum_{r=0}^{\infty} \left(\frac{\hbar}{2}\right)^{2r+1} \frac{(-1)^r}{(2r+1)!} \sum_{s=0}^{2r+1} \binom{2r+1}{s}(\alpha_V\beta_P)^{2r+1-s}(-\alpha_P\beta_V)^s\right]D(\alpha+\beta)$$

$$= \sum_{r=0}^{\infty} \sum_{s=0}^{2r+1} \sum_{j=0}^{\infty} \sum_{k=0}^{j} \sum_{m=0}^{j-k} \sum_{n=0}^{k} \left(\frac{\hbar^2}{4}\right)^r \frac{(-1)^{r+s}}{s!(2r+1-s)!} \frac{\alpha_P^{s+j-k-m} \alpha_V^{2r+1-s+k-n} \beta_P^{2r+1-s+m} \beta_V^{s+n}}{m!(j-k-m)!n!(k-n)!} G^{j-k,k}, \qquad (12)$$

whereas, for the second one, the expansion is given by

$$(\alpha_P\beta_V - \alpha_V\beta_P)D(\alpha)D(\beta)$$

$$= \sum_{j=0}^{\infty} \sum_{k=0}^{j} \sum_{m=0}^{\infty} \sum_{n=0}^{m} \frac{G^{j-k,k}G^{m-n,n}}{k!(j-k)!n!(m-n)!}$$

$$\times (\alpha_P^{j-k+1} \alpha_V^k \beta_P^{m-n} \beta_V^{n+1} - \alpha_P^{j-k} \alpha_V^{k+1} \beta_P^{m-n+1} \beta_V^n). \qquad (13)$$

Since (11) must be satisfied for all values of α and β we find that the coefficients in front of each of the powers of various α's and β's must be equal. By direct comparison we then obtain the Poisson bracket between our quantum variables. Making the convenient substitutions $a = w - x$, $b = x$, $c = y - z$, and $d = z$, and combining the factorials into binomial coefficients the result reads,

$$\{G^{a,b}, G^{c,d}\} = adG^{a-1,b}G^{c,d-1} - bcG^{a,b-1}G^{c-1,d}$$

$$+ \sum_{r=0}^{\infty} \sum_{s=0}^{2r+1} 2\hbar^{2r}(-1)^{r+s}C_{ad}^s C_{bc}^{2r+1-s}$$

$$\times G^{a+c-2r-1,b+d-2r-1}. \qquad (14)$$

Finally we make the replacement $n = 2r + 1$, noting that in the summation over r the only nonzero terms occur when $2r + 1 < \text{Min}(a + c, b + d, a + b, c + d)$, which gives us (5).

III. ALGEBRAIC IMPLEMENTATION

We have written two different codes in MATHEMATICA in order to obtain the Poisson brackets between any two generic moments. The first code works iteratively, whereas the second one makes use of the general formula (5). The results agree for all orders checked (up to 14th) but the second code is much more efficient. This can be clearly seen in Fig. 2, where we have plotted the timing of both
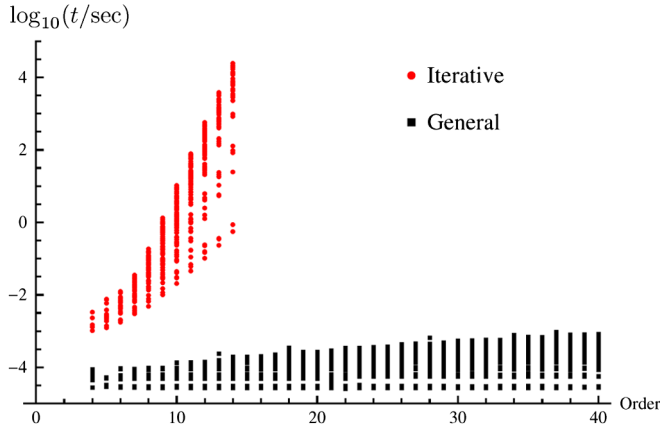
FIG. 2 (color online). In this figure we compare the timing of computing the Poisson brackets between any two moments with the code working iteratively as well as the one that makes use of the general formula (5). The time, shown in a logarithmic scale (to base 10), has been measured in seconds. The order plotted in the graphics corresponding to a bracket $\{G^{a,b}, G^{c,d}\}$ has been defined as the sum of all the indices: $a + b + c + d$. Note the exponential increase of the timing for the recursive code, whereas the computations with the general code are kept in the order of 10^{-4} seconds up to the considered order. There are $N \equiv (n + 1)(n + 2)/2 - 3$ different moments with an order less or equal to n, where the subtraction of 3 comes from the fact that the order 0 and 1 moments are trivial; they can be combined into $N(N + 1)/2$ different Poisson brackets. In the case of the recursive (general) code, the 33 (228) moments up to order seven (20) have been considered, and in the plot the timing for their corresponding 561 (26 106) independent Poisson brackets are drawn.

codes to compute several Poisson brackets. The timing of the recursive code increases exponentially with the order of the considered Poisson bracket, whereas the general code allows us to obtain high-order results in a very short time. This fact shows the importance of the general formula (5) from a practical point of view.

In the following we briefly explain how the recursive code works. Making use of the binomial identity, the expression for the moments can be written as,

$$G^{a,b} = \sum_{k=0}^{a} \sum_{n=0}^{b} (-1)^{a+b-k-n} \binom{a}{k} \binom{b}{n}$$
$$\times P^{a-k} V^{b-n} \langle \hat{P}^k \hat{V}^n \rangle_{\text{Weyl}}. \quad (15)$$

On the other hand, we also have found that the Weyl ordering can be given as a linear combination of expectation values with a predefined order, for any operators $\hat{A}$ and $\hat{B}$ with a c-number commutator,

$$\langle \hat{A}^k \hat{B}^n \rangle_{\text{Weyl}} = \sum_{d=0}^{\text{Min}(k,n)} [\hat{B}, \hat{A}]^d C_{kn}^d \langle \hat{A}^{k-d} \hat{B}^{n-d} \rangle, \quad (16)$$

where the coefficients C_{kn}^d have been defined in (7). Hence, for our case of interest, we can write either

$$\langle \hat{P}^k \hat{V}^n \rangle_{\text{Weyl}} = \sum_{d=0}^{\text{Min}(k,n)} (i\hbar)^d C_{kn}^d \langle \hat{P}^{k-d} \hat{V}^{n-d} \rangle, \quad (17)$$

or,

$$\langle \hat{P}^k \hat{V}^n \rangle_{\text{Weyl}} = \sum_{d=0}^{\text{Min}(k,n)} (-i\hbar)^d C_{kn}^d \langle \hat{V}^{n-d} \hat{P}^{k-d} \rangle. \quad (18)$$

In order to obtain the Poisson brackets between different moments iteratively we make use of the definition of the moments in the form,

$$G^{a,b} = \sum_{k=0}^{a} \sum_{n=0}^{b} \sum_{d=0}^{\text{Min}(k,n)} (-i\hbar)^d (-1)^{a+b-k-n} \binom{a}{k} \binom{b}{n}$$
$$\times C_{kn}^d P^{a-k} V^{b-n} \langle \hat{V}^{n-d} \hat{P}^{k-d} \rangle. \quad (19)$$

For computing $\{G^{a,b}, G^{c,d}\}$ we then use the properties of the Poisson brackets as well as of the commutator until all operator terms reduce to the simple commutator between the isolated operators $\hat{V}$ and $\hat{P}$.

IV. A MASSLESS SCALAR FIELD WITH COSMOLOGICAL CONSTANT

As an application of high-order quantum back-reaction we now introduce a cosmological model with a regime of large moments: an isotropic spatially flat universe filled with a free, massless scalar ϕ (with momentum p_ϕ) and a positive cosmological constant $\Lambda > 0$. From the Friedmann equation

$$\left(\frac{a'}{a}\right)^2 = \frac{4\pi G}{3} \frac{p_\phi^2}{a^6} + \Lambda, \quad (20)$$

we obtain, ignoring constant factors for the sake of compactness, $p_\phi = a^2 \sqrt{a'^2 - \Lambda a^2}$ where the prime is the derivative with respect to cosmological time. The square root may take both signs, corresponding to expanding and contracting cosmological solutions. We will choose the positive sign in order to analyze expanding universe models approaching large volume, as they remain in a low-curvature regime. The opposite sign, if desired, could be easily included since it would just invert the sign of the constant of motion p_ϕ [which will be the deparameterized classical Hamiltonian of our system (22)] as well as the effective Hamiltonian (23) below. Therefore, from the expanding solutions we show it will be straightforward to get their contracting counterparts just by performing a time reversal.

We rewrite p_ϕ as

$$p_\phi = (1 - x)V \sqrt{P^2 - \Lambda[(1 - x)V]^{(1+2x)/(1-x)}} \quad (21)$$

in terms of canonical gravitational variables $V = (1 - x)^{-1} a^{2-2x}$ and $P = -a^{2x} a'$. The parameter x characterizes different cases of lattice refinement of an

underlying discrete state; see [11,12]. The quantum dynamics (Wheeler-DeWitt type) that will be implemented in this paper is insensitive to the change of this discreteness parameter. However, some values lead to advantages in the solution procedure, as we will make use of below. Moreover, it is useful to keep the parameter in the definition of canonical variables in order to facilitate possible applications to loop quantum cosmology in the near future, where this parameter will become relevant.

The system is simplest to deal with for $x = -1/2$, in which case V is proportional to the volume, because p_ϕ, which can be thought of as the Hamiltonian for evolution in internal time ϕ, is then linear in V. For a negative cosmological constant, the effective evolution coming from a quantization of (21) has been solved and analyzed in [13], some of whose formulas apply here as well. (For numerical wave-function evolution of this model with $\Lambda < 0$, see [14].) For $\Lambda < 0$, however, the moments do not grow large at large volume, and the volume is bounded by recollapse. These two features are not present for $\Lambda > 0$, making an analysis of high-order moments necessary, the topic of this article.

From now on we use $x = -1/2$, which implies

$$p_\phi = H = \frac{3}{2} V \sqrt{P^2 - \Lambda} \qquad (22)$$

as the Hamiltonian of the deparametrized system. Since the dependence of the classical Hamiltonian on V is linear, we will only obtain terms of the form $G^{a,0}$ and $G^{a,1}$ in the quantum Hamiltonian and we have the closed expression,

$$H_Q = \frac{3}{2} V \sqrt{P^2 - \Lambda} + \frac{3}{2} \sqrt{\Lambda} \sum_{n=2}^{\infty} \frac{\Lambda^{-n/2}}{n!} [V T_n(P/\sqrt{\Lambda}) G^{n,0}$$
$$+ n\sqrt{\Lambda} T_{n-1}(P/\sqrt{\Lambda}) G^{n-1,1}], \qquad (23)$$

where we have defined

$$T_n(x) := \frac{d^n}{dx^n} \sqrt{x^2 - 1}. \qquad (24)$$

Explicitly, the moments appearing here are

$$G^{n,0} := \langle(\hat{P} - \langle\hat{P}\rangle)^n\rangle,$$

$$G^{n-1,1} := \frac{1}{n} \sum_{i=0}^{n-1} \langle(\hat{P} - \langle\hat{P}\rangle)^i(\hat{V} - \langle\hat{V}\rangle)(\hat{P} - \langle\hat{P}\rangle)^{n-1-i}\rangle.$$

Hamiltonian (23) will describe the semiclassical behavior of the Wheeler-DeWitt quantization of this system.

Equations of motion for V and P are derived as in any Hamiltonian system, noting that the expectation values Poisson commute with any quantum variable. This gives

$$\dot{V} = \frac{3}{2} V \frac{P}{\sqrt{P^2 - \Lambda}} + \frac{3}{2} \sum_{n=2}^{\infty} \frac{\Lambda^{-n/2}}{n!} [V T_{n+1}(P/\sqrt{\Lambda}) G^{n,0}$$
$$+ n\sqrt{\Lambda} T_n(P/\sqrt{\Lambda}) G^{n-1,1}], \qquad (25)$$

$$\dot{P} = -\frac{3}{2} \sqrt{P^2 - \Lambda} - \frac{3}{2} \sqrt{\Lambda} \sum_{n=2}^{\infty} \frac{\Lambda^{-n/2}}{n!} T_n(P/\sqrt{\Lambda}) G^{n,0}, \qquad (26)$$

where dot stands for derivatives with respect to ϕ and we have made use of the fact that

$$\{V, T_n(P/\sqrt{\Lambda})\} = \frac{1}{\sqrt{\Lambda}} T_{n+1}(P/\sqrt{\Lambda}). \qquad (27)$$

Equations of motion for the quantum variables can also be derived from Poisson relations between them

$$\dot{G}^{r,s} = \frac{3}{2} \sqrt{\Lambda} \sum_{n=2}^{\infty} \frac{\Lambda^{-n/2}}{n!} [V T_n(P/\sqrt{\Lambda})\{G^{r,s}, G^{n,0}\}$$
$$+ n\sqrt{\Lambda} T_{n-1}(P/\sqrt{\Lambda})\{G^{r,s}, G^{n-1,1}\}]. \qquad (28)$$

In fact, this highly coupled system of infinitely many variables is extremely complicated to solve, and we will try to analyze it by means of truncations to finitely many variables which include the expectation values and only low order quantum variables.

A. Vanishing Λ

For $\Lambda = 0$, we obtain the harmonic model of [15] for which all equations decouple:

$$\dot{V} = \frac{3}{2} V, \qquad (29)$$

$$\dot{P} = -\frac{3}{2} P, \qquad (30)$$

$$\dot{G}^{ab} = \frac{3}{2}(b - a)G^{ab}. \qquad (31)$$

There is no quantum back-reaction, and all equations can easily be solved:

$$V(\phi) = V_0 \exp[\tfrac{3}{2}(\phi - \phi_0)], \qquad (32)$$

$$P(\phi) = P_0 \exp[-\tfrac{3}{2}(\phi - \phi_0)], \qquad (33)$$

$$G^{ab}(\phi) = G_0^{ab} \exp[\tfrac{3}{2}(b - a)(\phi - \phi_0)]. \qquad (34)$$

B. Classical equations

To classical order, i.e., assuming all moments to vanish, we obtain analytical solutions

$$P_{\text{classical}}(\phi) = P_0 \cosh(3(\phi - \phi_0)/2)$$
$$- \sqrt{P_0^2 - \Lambda} \sinh(3(\phi - \phi_0)/2), \qquad (35)$$

$V_{\text{classical}}(\phi)$

$$= V_0 \frac{\sqrt{P_0^2 - \Lambda}}{\sqrt{P_0^2 - \Lambda}\cosh(3(\phi - \phi_0)/2) - P_0 \sinh(3(\phi - \phi_0)/2)},$$

(36)

where V_0 and P_0 are the value of the expectation values at the initial time ϕ_0. At the time when $\phi_{\text{div}} := \phi_0 + 2/3\tanh^{-1}(\sqrt{P_0^2 - \Lambda}/P_0)$ the volume $V_{\text{classical}}(\phi)$ diverges, and $\sqrt{P_{\text{classical}}(\phi_{\text{div}})^2 - \Lambda} = 0$.

C. Second order

To understand whether quantum effects can be important in this large-volume regime of small curvature (if Λ is small), we will analytically solve (under certain approximations) the equations of motion for second-order quantum variables, i.e. fluctuations $G^{2,0}$, $G^{0,2}$ and the covariance $G^{1,1}$. To this order, ignoring higher moments, we have a quantum Hamiltonian

$$H_Q = \frac{3}{2} V\sqrt{P^2 - \Lambda} - \frac{3}{4}\Lambda\frac{V}{(P^2 - \Lambda)^{3/2}}G^{2,0}$$

$$+ \frac{3}{2}\frac{P}{\sqrt{P^2 - \Lambda}}G^{1,1}.$$

(37)

Using the Poisson bracket relations

$$\{G^{0,2}, G^{1,1}\} = 2G^{0,2}, \qquad \{G^{0,2}, G^{2,0}\} = 4G^{1,1},$$

$$\{G^{1,1}, G^{2,0}\} = 2G^{2,0},$$

(38)

the moments satisfy the equations of motion,

$$\dot{G}^{2,0} = -3\frac{P}{\sqrt{P^2 - \Lambda}}G^{2,0},$$

(39)

$$\dot{G}^{1,1} = -\frac{3}{2}\Lambda\frac{V}{(P^2 - \Lambda)^{3/2}}G^{2,0},$$

(40)

$$\dot{G}^{0,2} = -3\Lambda\frac{V}{(P^2 - \Lambda)^{3/2}}G^{1,1} + 3\frac{P}{\sqrt{P^2 - \Lambda}}G^{0,2}.$$

(41)

1. Expectation values as background solutions

As a first approximation, we can use the classical solutions for V and P as some kind of background on which the quantum variables evolve. From the resulting solutions we then determine whether quantum back-reaction effects by quantum variables on expectation values are significant.

The equations for fluctuations to this level of truncation are not strongly coupled, which allows us to solve for all of them by integrations. For $G^{2,0}$, we obtain

$$G^{2,0}(\phi) = G^{2,0}(\phi_0)(\cosh(3(\phi - \phi_0)/2)$$

$$- \frac{P_0}{\sqrt{P_0^2 - \Lambda}}\sinh(3(\phi - \phi_0)/2))^2, \quad (42)$$

which then allows us to solve for $G^{1,1}$ and, in turn, $G^{0,2}$. We do not present these solutions here (which can be found from [13] by changing the sign of Λ), but note that (41) can be written as

$$\frac{d}{d\phi}\left(\frac{G^{0,2}}{V_{\text{classical}}^2}\right) = -3\Lambda\frac{G^{1,1}}{V_{\text{classical}}(P^2 - \Lambda)^{3/2}}.$$

(43)

(Within the second-order approximation, we could replace $V_{\text{classical}}$ with V in this equation up to terms of the form $G^{0,2}G^{2,0}$ and $G^{0,2}G^{1,1}$.) This shows that the evolution of volume fluctuations relative to volume is determined by the covariance $G^{1,1}$. For an unsqueezed state, we would have $G^{1,1} = 0$ and squared volume fluctuations would be proportional to the total volume. However, even if we start with an unsqueezed initial state, squeezing would develop over time since $\dot{G}^{1,1}$ is nonzero. In this way, the precise state has to be analyzed to understand the long-term evolution of fluctuations.

2. Coupled equations

The solution (42) for $G^{2,0}$, compared with (36), shows that curvature fluctuations to second order vanish where V diverges. Thus, also $G^{0,2}$ has to diverge there in order to respect the uncertainty relation. The approach to zero is the same for $\sqrt{G^{2,0}}$, $1/V$ and $\sqrt{P^2 - \Lambda}$, which we can use to check whether quantum back-reaction is important. Writing equations of motion for expectation values to the order where coupling terms to fluctuations appear, we obtain

$$\dot{P} = -\frac{3}{2}\sqrt{P^2 - \Lambda} + \frac{3}{4}\Lambda\frac{G^{2,0}}{(P^2 - \Lambda)^{3/2}},$$

(44)

$$\dot{V} = \frac{3}{2}\frac{VP}{\sqrt{P^2 - \Lambda}} + \frac{9}{4}\Lambda\frac{VPG^{2,0}}{(P^2 - \Lambda)^{5/2}} - \frac{3}{2}\Lambda\frac{G^{1,1}}{(P^2 - \Lambda)^{3/2}},$$

(45)

which now forms a coupled set of five differential equations if we include $G^{0,2}$. When V diverges, coupling terms due to quantum back-reaction cannot be ignored. In $\dot{P}$, for instance, the coupling term diverges, and in fact dominates the classical term, since $G^{2,0}$ vanishes like $P^2 - \Lambda$, and also $\dot{V}$ has diverging coupling terms. Even the truncation used here, which does include some quantum corrections, is not consistent at this point because one has to expect that further correction terms by higher moments become large, too. Nevertheless, in the approach to the divergence of V, correction terms should become relevant one by one, depending on their moment order. Thus, it is of interest to

analyze the coupled system written here to second order in the moments before proceeding to higher orders.

We first focus on the system given by the Eqs. (44) for $\dot{P}$ and (39) for $\dot{G}^{2,0}$ since these two equations are coupled only with each other. If we divide $\dot{P}$ by $\dot{G}^{2,0}$, we obtain the differential equation

$$\frac{dP}{dG^{2,0}} = \frac{1}{2}\frac{P^2 - \Lambda}{PG^{2,0}} - \frac{1}{4}\frac{\Lambda}{P(P^2 - \Lambda)}, \qquad (46)$$

for $P(G^{2,0})$ or, in a simpler form,

$$\frac{d(P^2 - \Lambda)}{d\log G^{2,0}} = P^2 - \Lambda - \frac{1}{2}\frac{\Lambda}{P^2 - \Lambda}G^{2,0}. \qquad (47)$$

This equation of the form

$$f'(x) = f(x) - \frac{1}{2}\Lambda\frac{e^x}{f(x)}$$

can be solved by

$$f(x) = \sqrt{ce^{2x} + \Lambda e^x}$$

with an integration constant c. In this way, we derive the exact second-order relations

$$P = \sqrt{\Lambda + \sqrt{c(G^{2,0})^2 + \Lambda G^{2,0}}}, \qquad (48)$$

$$\sqrt{P^2 - \Lambda} = \sqrt[4]{c(G^{2,0})^2 + \Lambda G^{2,0}}. \qquad (49)$$

We can use these relations to solve the equations of motion for $P(\phi)$ and $G^{2,0}(\phi)$, but the resulting differential equations are complicated. For $G^{2,0}$, for instance, the differential equation is

$$\dot{G}^{2,0} = -3\frac{P}{\sqrt{P^2 - \Lambda}}G^{2,0}$$

$$= -3\sqrt{(G^{2,0})^2 + \frac{\Lambda G^{2,0}}{\sqrt{c + \Lambda/G^{2,0}}}}. \qquad (50)$$

Fortunately, as we will see in the next subsection, already the relation $P(G^{2,0})$ has interesting implications regarding the quantum back-reaction problem. We will continue using (50) in the next subsection, but first note that further analysis, at least numerically, of the truncated second-order system could be facilitated by an explicit decoupling of the equations. We have already provided direct equations for P and $G^{2,0}$ which we can assume to be solved by integrations. Further equations are then still coupled amongst each other, but different combinations are decoupled. First, we combine $\dot{V}$ and $\dot{G}^{1,1}$ to

$$\frac{d}{d\phi}\left(\frac{G^{1,1}}{V}\right) = -\frac{3}{2}\Lambda\frac{G^{2,0}}{(P^2 - \Lambda)^{3/2}} - \frac{3}{2}\frac{P}{\sqrt{P^2 - \Lambda}}\frac{G^{1,1}}{V}$$

$$- \frac{9}{4}\Lambda\frac{P}{(P^2 - \Lambda)^{5/2}}G^{2,0}\frac{G^{1,1}}{V}$$

$$+ \frac{3}{2}\Lambda\frac{1}{(P^2 - \Lambda)^{3/2}}\left(\frac{G^{1,1}}{V}\right)^2 \qquad (51)$$

which is already decoupled from the rest. Once $G^{1,1}/V$ has been solved for, (45) presents an uncoupled differential equation for V, and we can finally integrate (41) for $G^{0,2}$.

3. Strength of quantum back-reaction

The term $\Lambda G^{2,0}$ in (49) arises through the quantum back-reaction in the evolution equation for P (44). If this term is ignored, we reproduce the previous approximated solution $G^{2,0} = G^{2,0}(\phi_0)(P^2 - \Lambda)/(P_0^2 - \Lambda)$, which follows from (35) and (42). Hence, comparison shows that the integration constant is proportional to $c \sim (P_0^2 - \Lambda)^2/[G^{2,0}(\phi_0)]^2$ if initial values are imposed where back-reaction is weak. Starting with a semiclassical initial state, for some time we will have $G^{2,0}(\phi) \sim G^{2,0}(\phi_0)$ and the term $\Lambda G^{2,0}$ can indeed be ignored compared to the classical parameter $(P_0^2 - \Lambda)^2$ in (49). (The value of $P_0^2 - \Lambda$ cannot vanish under the stated assumptions, for we already know that back-reaction terms would then be large at ϕ_0.) But as we approach the divergence of V, we have seen that $G^{2,0}$ according to the lowest order solution (42) would tend to zero. In this regime, the new term $\Lambda/G^{2,0}$ in (50) will eventually dominate over the constant c. This is another demonstration of the fact that quantum back-reaction is important at this place.

For $c = 0$, i.e. in the strong quantum back-reaction regime where $\Lambda/G^{2,0}$ dominates, we can find a solution for (50). The combination $h(\phi) := \sqrt[4]{G^{2,0}(\phi)/\Lambda}$ csc satisfies a simple differential equation solved by $G^{2,0}(\phi) = \Lambda\sinh^4(3(\phi - \phi_0)/4)$. The higher power compared to the solution (42) in the absence of back-reaction again indicates that quantum back-reaction becomes important at large volume.

Turning now to V, we can confirm that the quantum back-reaction term does change its behavior of divergence. In (45), the dominant back-reaction term involves $G^{2,0}$ rather than $G^{1,1}$. Ignoring quantum back-reaction in the solution for $G^{2,0}$, we would have

$$\frac{\dot{V}}{V} \sim \frac{3}{2}\frac{P}{\sqrt{P^2 - \Lambda}} + \frac{9}{4}\frac{\Lambda P}{\sqrt{c}(P^2 - \Lambda)^{3/2}}.$$

The second term is subdominant. Quantum back-reaction in the solution for $G^{2,0}$, on the other hand, implies a stronger divergence as can be seen by using relation (48) for $c = 0$, since we now have

$$\frac{\dot{V}}{V} \sim \frac{15}{4} \frac{P}{\sqrt{P^2 - \Lambda}}.$$

Here, the quantum back-reaction term for V has the same form as the classical term, which have thus be combined. The prefactor of the right-hand side becomes larger than classically once quantum back-reaction is included, strengthening the divergence of V.

One may conjecture that, with all quantum corrections from the complete series of moments, the divergence of V would disappear. This is suggested by the fact that a self-adjoint Hamiltonian would provide unitary evolution in which the wave function remains well-defined throughout the point where the classical V diverges, and even beyond that point. In the model considered, the Hamiltonian for ϕ-evolution is not essentially self-adjoint but has several inequivalent self-adjoint extensions [16]. While subtle issues of self-adjoint extensions of operators usually do not play a large role in effective equations, provided that consistent truncations are possible, the point where V diverges classically requires all moments to be taken into account. With infinitely many independent variables, coupling terms have to be arranged in a precise manner, which can reflect issues of self-adjoint extensions. When all moments are taken into account in a way corresponding to unitary evolution of the corresponding wave function, well-defined equations for expectation values and the moments may result. This supports the conjecture that the classical divergence might be removed by an interplay of all moments, but a verification in this highly coupled system is complicated. (It could, in fact, happen that wave functions evolve out of the domain of definition of the unbounded operator $\hat{V}$, and then directly reenter. Thus, it is not obvious that equations for expectation values $\langle \hat{V} \rangle$ must be well-defined at all times. Another example which indicates caution against applying arguments of self-adjointness for the behavior of expectation values is the upside-down harmonic oscillator. Its Hamiltonian is not essentially self-adjoint and allows different self-adjoint extensions, depending on the boundary conditions at infinity where wave packets are reflected. However, the Hamiltonian is also quadratic, and no quantum back-reaction results. Effective equations are automatically truncated without implementing any approximation; the evolution of moments to finite order just does not depend on what self-adjoint extension is used.)

We will probe the divergence of V further by the numerics of high-order moments. For now, conclusions one can draw already from the analysis presented so far are:

(i) Quantum back-reaction is essential at large volume in the presence of a positive cosmological constant, even though one would expect it to be a semiclassical regime of small curvature if Λ is small.

(ii) While a wave packet in a V-representation may not show large deviations from the classical trajectory, this is only because volume fluctuations grow and are larger than deviations from the classical trajectory. Nevertheless, as volume fluctuations diverge, deviations from the classical trajectory can be large. Equations including quantum back-reaction clearly show that correction terms cannot be ignored. Quantum back-reaction seems to strengthen the divergence of V rather than triggering a recollapse.

(iii) Corrections are more visible for curvature P since its fluctuations approach zero while also here quantum back-reaction terms in the equations of motion are relevant. Thus, deviations from the classical trajectory build up and, unlike for V, are not covered by a broad wave function if a P-representation is used.

(iv) All state parameters matter for the spreading behavior and for the exact size of quantum corrections. A state may be assumed to be unsqueezed initially, setting $G^{1,1}(\phi_0) = 0$, but correlations will build up over time.

D. Third order

At third or higher orders, the equations of motion not only become longer; there is also a new feature in the Poisson relations which we illustrate here. Some examples of third-order moments are

$$G^{3,0} = \langle \hat{P}^3 \rangle - 3P G^{2,0} - P^3,$$

$$G^{2,1} = \frac{1}{3}\langle \hat{V}\hat{P}^2 + \hat{P}\hat{V}\hat{P} + \hat{P}^2\hat{V} \rangle - 2P G^{1,1} - V G^{2,0} - P^2 V,$$

$$G^{1,2} = \frac{1}{3}\langle \hat{P}\hat{V}^2 + \hat{V}\hat{P}\hat{V} + \hat{V}^2\hat{P} \rangle - 2V G^{1,1} - P G^{0,2} - V^2 P.$$

The Poisson brackets of second-order with third-order moments are of third-order form, for instance:

$$\{G^{0,2}, G^{3,0}\} = 6G^{2,1}, \qquad \{G^{0,2}, G^{2,1}\} = 4G^{1,2},$$

$$\{G^{1,1}, G^{3,0}\} = 3G^{3,0}, \qquad \{G^{1,1}, G^{2,1}\} = G^{2,1},$$

$$\{G^{2,0}, G^{2,1}\} = -2G^{3,0}, \qquad \{G^{2,0}, G^{3,0}\} = 0,$$

where only the ones needed for evolution in our cosmological system were written. Two third-order moments in a Poisson bracket, on the other hand, show a different behavior: They produce a term of higher order (fourth) as well as products of second-order moments, which are to be considered as being of fourth order in the hierarchy. This behavior of the Poisson structure has consequences for the truncation of equations of motion.

Unlike for second order, (38), there is a difference between expanding the Hamiltonian to third order and then deriving equations of motion, and expanding the equations of motion (obtained from an expanded Hamiltonian or the whole series in $\hbar$) to third order. In particular, moments of third order in the Hamiltonian produce moments of fourth order in the equations of motion for third-order moments. This would result in a

complete set if also equations of motion for fourth-order moments are included. This problem does not arise if one first computes equations of motion and expands those to third (or any) order which is anyway more suitable because it is the equations of motion which we are primarily interested in. We illustrate this feature by the following evolution equations, computed from the third-order Hamiltonian:

$$\dot{P} = -\frac{3}{2}\sqrt{P^2 - \Lambda} + \frac{3}{4}\Lambda\frac{G^{2,0}}{(P^2 - \Lambda)^{3/2}}$$
$$- \frac{3}{4}\frac{\Lambda P}{(P^2 - \Lambda)^{5/2}}G^{3,0}, \tag{52}$$

$$\dot{V} = \frac{3}{2}\frac{VP}{\sqrt{P^2 - \Lambda}} + \frac{9}{4}\Lambda^2\frac{VPG^{2,0}}{(P^2 - \Lambda)^{5/2}} - \frac{3}{2}\Lambda^2\frac{G^{1,1}}{(P^2 - \Lambda)^{3/2}}$$
$$- \frac{3}{4}\Lambda^2\frac{V(4P^2 + \Lambda)}{(P^2 - \Lambda)^{7/2}}G^{3,0} + \frac{9}{4}\Lambda^2\frac{P}{(P^2 - \Lambda)^{5/2}}G^{2,1}, \tag{53}$$

$$\dot{G}^{2,0} = -3\frac{P}{\sqrt{P^2 - \Lambda}}G^{2,0} + \frac{9}{4}\frac{\Lambda}{(P^2 - \Lambda)^{3/2}}G^{3,0}, \tag{54}$$

$$\dot{G}^{1,1} = -\frac{3}{2}\frac{\Lambda V}{(P^2 - \Lambda)^{3/2}}G^{2,0} + \frac{9}{4}\frac{\Lambda PV}{(P^2 - \Lambda)^{5/2}}G^{3,0}$$
$$- \frac{3}{4}\frac{\Lambda}{(P^2 - \Lambda)^{3/2}}G^{2,1}, \tag{55}$$

$$\dot{G}^{0,2} = -3\frac{\Lambda V}{(P^2 - \Lambda)^{3/2}}G^{1,1} + 3\frac{P}{\sqrt{P^2 - \Lambda}}G^{0,2}$$
$$+ \frac{9}{4}\frac{\Lambda VP}{(P^2 - \Lambda)^{5/2}}G^{3,0} - \frac{3}{4}\frac{\Lambda}{(P^2 - \Lambda)^{3/2}}G^{2,1}. \tag{56}$$

If we truncate the Hamiltonian (and hence the equations of motion) to a given order, the equations of motion for quantum variables involve higher order moments, as shown in the following equations to third order in moments,

$$\dot{G}^{3,0} = -\frac{9}{2}\frac{P}{\sqrt{P^2 - \Lambda}}G^{3,0} + \frac{9}{4}\frac{\Lambda}{(P^2 - \Lambda)^{3/2}}((G^{2,0})^2 - G^{4,0}), \tag{57}$$

$$\dot{G}^{2,1} = -\frac{3}{2}\Lambda\frac{V}{(P^2 - \Lambda)^{3/2}}G^{3,0} + \frac{9}{4}\frac{\Lambda PV}{(P^2 - \Lambda)^{5/2}}((G^{2,0})^2 - G^{4,0})$$
$$+ \frac{3}{2}\frac{P}{\sqrt{P^2 - \Lambda}}G^{2,1}, \tag{58}$$

$$\dot{G}^{1,2} = -3\Lambda\frac{V}{(P^2 - \Lambda)^{3/2}}G^{2,1} - \frac{9}{2}\frac{\Lambda VP}{(P^2 - \Lambda)^{5/2}}(G^{1,1}G^{2,0} - G^{3,1})$$
$$+ \frac{3}{2}\frac{P}{\sqrt{P^2 - \Lambda}}G^{2,1} - \frac{3}{4}\frac{\Lambda}{(P^2 - \Lambda)^{3/2}}(-4(G^{1,1})^2$$
$$+ G^{2,0}G^{0,2} + 3G^{2,2}), \tag{59}$$

$$\dot{G}^{0,3} = -\frac{9}{2}\Lambda\frac{V}{(P^2 - \Lambda)^{3/2}}G^{1,2} - \frac{27}{4}\frac{\Lambda VP}{(P^2 - \Lambda)^{5/2}}$$
$$\times (G^{0,2}G^{2,0} - G^{2,2}) + \frac{9}{2}\frac{P}{\sqrt{P^2 - \Lambda}}G^{0,3}$$
$$+ \frac{9}{2}\frac{\Lambda}{(P^2 - \Lambda)^{3/2}}(G^{1,1}G^{0,2} - G^{1,3}). \tag{60}$$

For consistency of the approximation one should eliminate in this third-order approximation all terms of quartic order, i.e. fourth-order moments, producing a closed set of equations. (One may eliminate terms quadratic in second-order moments as well, but they are anyway subdominant when the hierarchy is satisfied.) Truncating only the Hamiltonian to third order is thus not enough because the general Poisson bracket between two third-order moments produces terms of fourth order. (In general, the Poisson bracket of two moments of order n and m, respectively, produces terms of order $n + m - 2$ [see Eq. (5)]. Only for second order does this result in a closed Poisson algebra.) Consistently truncated equations of motion are produced if one truncates the Hamiltonian as well as the Poisson brackets to the order considered. An example to order five can be found in the Appendix.

E. High-order corrections

Because of the complicated structure of the equations at higher orders, analyzing them by analytical meanings is very hard. Hence we need to resort to numerical methods. In particular, in this subsection we will numerically solve the evolution equations, derived using computer algebra, up to 10th order. An important question is then what values to choose for all the 63 moments involved at initial time $\phi_0 = 0$. Here we will simply choose the initial state corresponding to an unsqueezed Gaussian pulse in the volume,

$$\Psi(\chi) = \frac{1}{\pi^{1/4}\sqrt{\sigma}}e^{-(\chi - V_0)^2/(2\sigma^2) + iP_0\chi/\hbar}. \tag{61}$$

While this state is very special in the space of all semiclassical moments, it already serves well to demonstrate several features of quantum evolution. A more detailed analysis of the large parameter space will appear elsewhere.

Using (19), the initial moments are then given by,

$$G^{a,b} \equiv \sum_{d=0}^{\text{Min}(a,b)} (-i\hbar)^a C_{ab}^d \int_{-\infty}^{\infty} d\chi \Psi^*(\chi)(\chi - V_0)^{b-d}$$
$$\times \left(\frac{d}{d\chi} - i\frac{P_0}{\hbar}\right)^{a-d} \Psi(\chi), \tag{62}$$

where $*$ denotes complex conjugation. This integral can be performed and happens to be vanishing except in those cases for which both a and b are even numbers,

$$G^{a,b} = \begin{cases} 2^{-(a+b)}\hbar^a \sigma^{b-a} \frac{a!b!}{(a/2)!(b/2)!} & \text{if } a \text{ and } b \text{ are even,} \\ 0 & \text{otherwise.} \end{cases}$$
$$\tag{63}$$

This state saturates the uncertainty relation, and we have that $\sigma \sim \Delta V = \sqrt{G^{2,0}} \sim O(\sqrt{\hbar})$, so the moments satisfy the semiclassical hierarchy. In our simulations, however, we have used $\hbar = 1$ in order to make implications for the behavior of back-reaction more clearly visible. Nevertheless, the features we point out have been verified also for smaller values of $\hbar$.

By this choice of initial values, the many-parameter family of all moments up to a given order is thus reduced to a 1-parameter family labeled by the volume spread σ. From this perspective, choosing a Gaussian initial state seems rather special and arbitrary; it is distinguished only by the simplicity of writing down a wave function. As the system evolves, the state will depart from Gaussian behavior, a property which can easily be seen by following the behavior of the moments. Before discussing the numerical results in this direction, we note that the choice of Gaussian moments as initial values can sometimes be dangerous also for numerical purposes. A Gaussian state saturates the uncertainty relations, and numerical errors may easily move the evolved moments to the wrong side of saturation. Depending on the dynamical system, the saturation surface may be unstable such that uncertainty relations may be violated after some stretch of numerical evolution, which at that stage could no longer be trusted. (See also [17] for a discussion of similar issues in small-volume regimes.) In the numerical evolutions shown here, the fact that uncertainty relations are maintained has explicitly been tested by monitoring the relevant combinations of the second-order moments. In particular, the final time of each evolution has been chosen as the last time where the convergence tests are obeyed.

Once an unsqueezed Gaussian is chosen as initial state, the only choice left is the value of σ. The system under consideration has no ground state, and thus there is no preferred value for σ as for instance the harmonic oscillator would suggest. For small initial fluctuations, which are related to σ by $\sigma \sim \Delta V \sim 1/\Delta P$, we just require that $1/P_0 \ll \sigma \ll V_0$ is satisfied for the initial values. Specifically, in all evolutions presented in this paper we take $V_0 = 1$, $P_0 = 10^4$ and $\sigma = 0.01$. This does not represent a high restriction since we have also performed numerical simulations for different larger values of the width ($\sigma = 1$, 100, 10^4) and the qualitative picture is not changed. Even so, the behavior of the system for values of $\sigma \lesssim 10^{-4}$ is completely different. In this case the corrections to the classical trajectories are very large from the very beginning and the approximation can not be regarded as valid. This happens because in the evolution Eqs. (25) and (26), the moments $G^{n-1,1}$ and $G^{n,0}$ appear. At the initial time ϕ_0 the former is zero, whereas the latter is of the order σ^{-n} for even n and vanishing for odd n. Hence, for very small σ, the initial time derivatives of V and P increase much with the considered order. This entails a completely different trajectory for the classical objects at each order and thus the approximation breaks down.

Finally, for the classical solutions (35) and (36) to exist, the cosmological constant must be in the interval $[0, P_0^2)$, so we have chosen three representative values: small $\Lambda = 1$, intermediate $\Lambda = 10^4$, and large $\Lambda = 9 \times 10^7$. These values are much higher than the observed one. Even so, since the model we adopt as an example is unphysical anyway, it would not be meaningful to have it clad in a physical guise by using the observational value for Λ. We use the mentioned values in order to bring out more clearly the properties we have found about high-order moments.

1. Numerical results

Let us first explain the behavior of the volume V. For the case of small and intermediate values of the cosmological constant, the evolution of the volume reproduces the classical one with small corrections at all orders. However, in the case of large cosmological constant we find that, at later times, the classical trajectory of the volume receives large quantum corrections, which make it diverge faster (see Fig. 3). In particular, we do not see any indication that quantum back-reaction may trigger a recollapse; instead, the classical divergence of the volume is enhanced by quantum corrections with each order. In Appendix A we provide a complete analysis of the convergence of our solutions at different orders by studying the relative corrections that the expectation value of the volume receives at each order. These results show that our effective analysis is valid (converges exponentially) at all considered times with a high precision.

Regarding the evolution of the moments there are two different behaviors. On the one hand, those $G^{i,j}$ with $(-1)^{i+j} = 1$ only show one branch; see the two characteristic examples shown in Fig. 4. That is, their evolution at different orders reproduce the same trajectory (for large values of the cosmological constant with small corrections). On the other hand, the moments with $(-1)^{i+j} = -1$ show two different branches. One of them always corresponds to the order $i + j$ and the other one to higher orders. This curious behavior is due to the fact that, in the latter case, when truncating the equations of motion
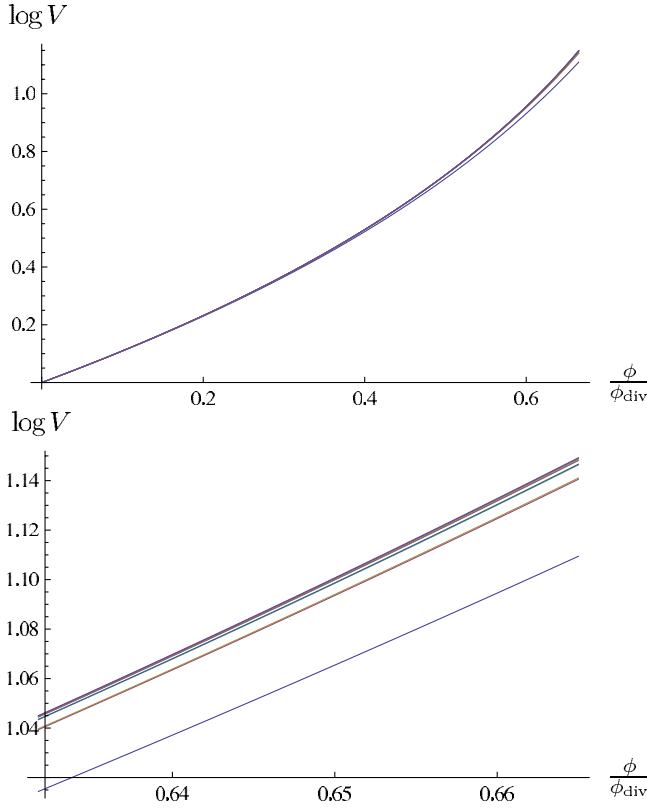
FIG. 3 (color online). The ten different evolutions of the volume V at each order for $\Lambda = 9 \times 10^7$. The lowest trajectory corresponds to the classical one. The values are increasing with the considered order in such a way that the largest trajectory is obtained at 10th order. For a more detailed analysis of the convergence, see Appendix A.

corresponding to this moment at order $i + j$, we neglect the contribution of certain moments that are initially nonvanishing. In the former case, for $G^{i,j}$ with $(-1)^{i+j} = 1$, all neglected moments in its equation of motion at order $i + j$ happen to be initially vanishing.

Before commenting on the collective behavior of different moments, it will be useful to remember the particular case with $\Lambda = 0$ where, as shown in Sec. IV A, analytic solutions for the moments at all orders can be obtained. In this case the evolution equations for the classical variables as well as for the quantum corrections are completely decoupled, and there is no quantum back-reaction. Using the exact solutions (34), the moments G^{ab} with $a > b$ are exponentially decreasing, whereas those with $a < b$ increase exponentially. On the other hand, the variables with $a = b$ are constants of motion. Note also that the combinations $\sqrt[i]{|G^{0,i}|}/V$ and $\sqrt[i]{|G^{i,0}|}/P$ remain constant under evolution. In Fig. 5 we show these objects for different values of the cosmological constant. It can be clearly seen how the trajectories depart from the constant behavior earlier when increasing the value of the cosmological constant. In this simple system one can easily construct many other constants of motion, e.g. $G^{a,b}/(P^a V^b)$.
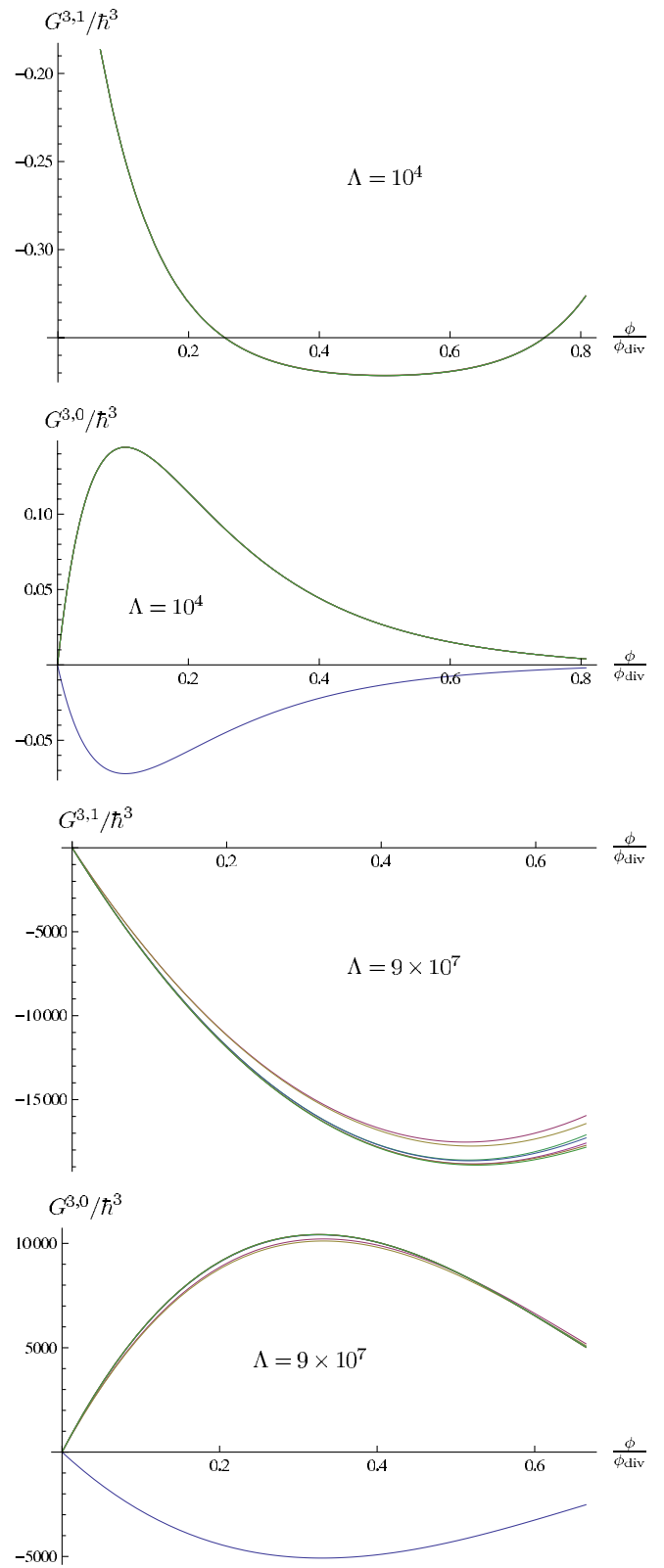

FIG. 4 (color online). An example with two different moments with one and two branches, respectively. For every moment $G^{i,j}$, the evolution at every order from $i + j$ to 10 is shown. The first two plots correspond to $\Lambda = 10^4$, whereas the other two represent the evolution of the same moments for $\Lambda = 9 \times 10^7$.
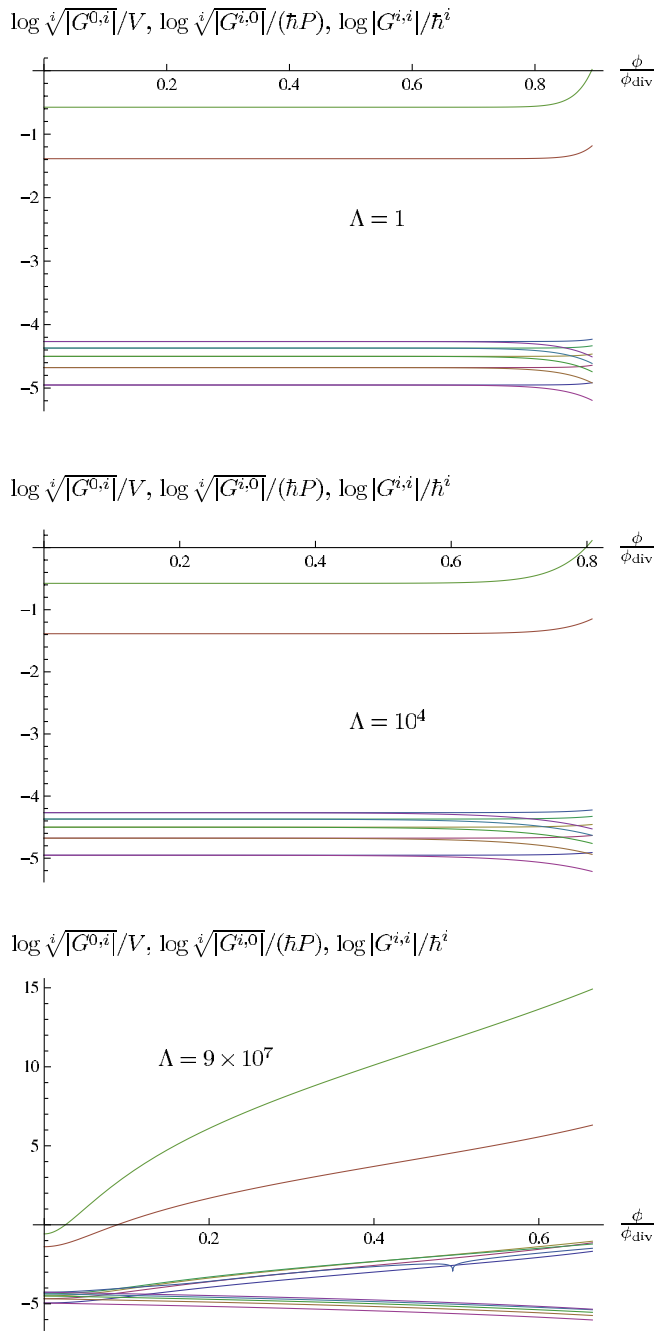
$\log \sqrt[i]{|G^{0,i}|}/V, \log \sqrt[i]{|G^{i,0}|}/(\hbar P), \log |G^{i,i}|/\hbar^i$

$\frac{\phi}{\phi_{\mathrm{div}}}$

$\Lambda = 1$

$\log \sqrt[i]{|G^{0,i}|}/V, \log \sqrt[i]{|G^{i,0}|}/(\hbar P), \log |G^{i,i}|/\hbar^i$

$\frac{\phi}{\phi_{\mathrm{div}}}$

$\Lambda = 10^4$

$\log \sqrt[i]{|G^{0,i}|}/V, \log \sqrt[i]{|G^{i,0}|}/(\hbar P), \log |G^{i,i}|/\hbar^i$

$\Lambda = 9 \times 10^7$

$\frac{\phi}{\phi_{\mathrm{div}}}$

FIG. 5 (color online). These figures show, in a logarithmic scale, objects that are constant in the case of a vanishing Λ. The plots correspond to the values $\Lambda = 1$, 10^4, and 9×10^7 respectively. In the first two graphics the moments are constant throughout evolution until very late times. On the other hand, for a large cosmological constant this behavior is violated from the very beginning. As a general feature, in all cases, once the moments are no longer constant, the quantities $\sqrt[i]{|G^{0,i}|}/V$ as well as $|G^{i,i}|$ happen to be increasing functions, whereas $\sqrt[i]{|G^{i,0}|}/P$ are decreasing. The different lines correspond, from largest to smallest value at the initial time, to the moments $G^{4,4}$, $G^{2,2}$, and then, with an equal initial value by pairs, to $(G^{10,0}, G^{0,10})$, $(G^{8,0}, G^{0,8})$, $(G^{6,0}, G^{0,6})$, $(G^{4,0}, G^{0,4})$, and $(G^{2,0}, G^{0,2})$.

Even though, for illustration, we will only consider those mentioned above.

Finally, in Figs. 6–9 we show the collective behavior of the different moments $G^{i,j}$. Essentially they have been divided in four groups depending on whether both i and j are even numbers or not and whether $i < j$ or $i > j$. This classification is inherited on the one hand from our chosen initial conditions, where the only nonvanishing moments are those with both i and j even, and on the other hand from the case without cosmological constant explained above, where the increasing or decreasing behavior of different moments also depends on the sign of $i - j$.

The increasing behavior of those moments $G^{i,j}$ with $i < j$ is obeyed also for nonvanishing values of the cosmological constant (see Figs. 7 and 9). On the other hand, in Figs. 6 and 8 the decreasing moments are plotted, but this behavior is violated as we move to higher values of the cosmological constant. As a general feature, in these plots it can also be observed that the evolution of different moments seems to be "slowed down," that is, everything (for example the instant when nearly all moments cross each other) happens later as one increases the value of the cosmological constant. This makes the hierarchy between different moments be retained for a longer time.

Another interesting issue is shown in the plots corresponding to the initially nonvanishing moments (Figs. 6 and 7): at late times those moments $G^{i,j}$ with the same number of $\hat{P}$, that is with a common index i, accumulate at a common value.

Finally, we note how the initially vanishing moments behave at the beginning of the simulations. As can be seen in Figs. 8 and 9, since the initial state of the system is not adapted to the equations of motion, these moments are excited very quickly to a "natural" value which more closely corresponds to a dynamical coherent state. The absolute value of a given moment $G^{i,j}$ immediately after this excitation, increases with the value of the cosmological constant Λ and approximately also with the difference $i - j$. This last dependence can be seen in the equations of motion. More explicitly, making use of the general formula (5) and our particular Hamiltonian (23) it can be checked that the time derivative of a moment $G^{i,j}$ is given as a linear combination of the following objects $\{G^{i,j-1}G^{k-1,0}, G^{i-1,j}G^{k-1,0}, G^{i,j-1}G^{k-2,1}, G^{i+k-n,j-n}, G^{i+k-1-n,j+1-n}\}$, where k must be summed from 2 to the order K at which we decide to truncate the Hamiltonian, and n corresponds to the sum over odd numbers that appears in Eq. (5). Taking into account the dependence of these objects on the Gaussian width σ at the initial time, it is straightforward to see that the initial time derivative of $G^{i,j}$ behaves like $\sigma^{-(K+i-j)}$.

2. Implications for state evolution

In Sec. IV C, several questions about the evolution of states has been suggested by the second-order analysis, but could not be answered without more general information
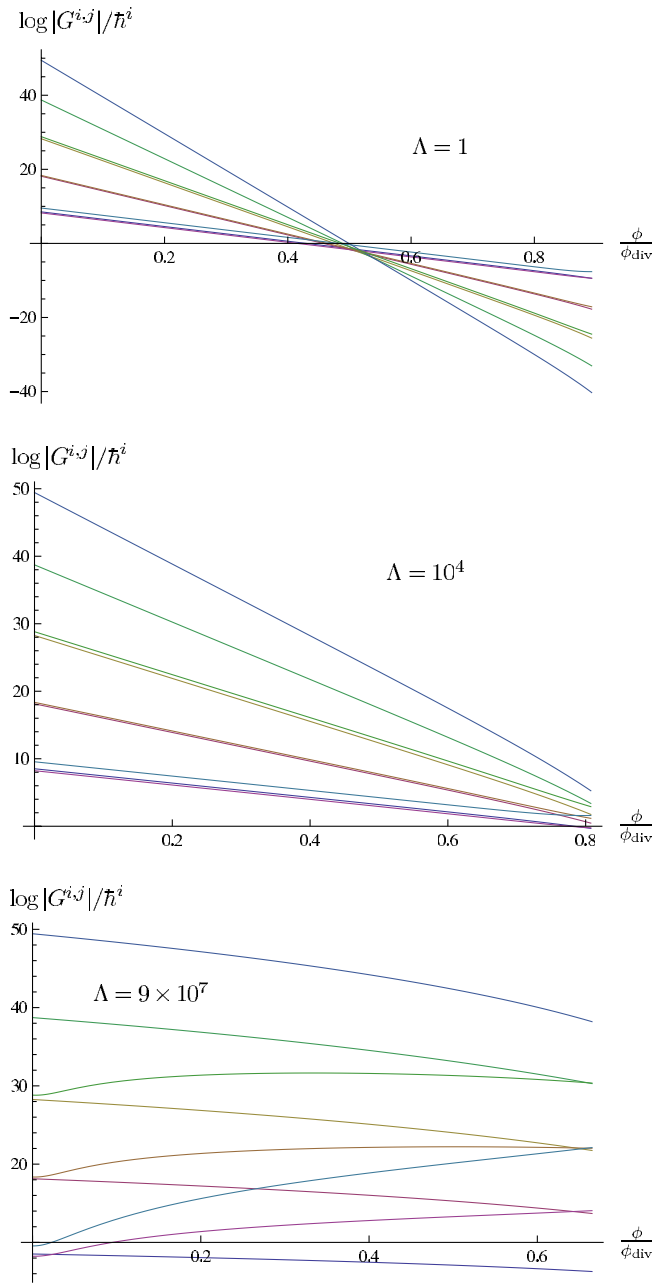
FIG. 6 (color online). This figure shows the evolution of the moments $G^{i,j}$ with $i > j$ and for both i and j even. Different plots correspond to the values $\Lambda = 1$, 10^4, and 9×10^7 respectively. In the first two plots we observe that the exponentially decaying behavior of these moments is maintained for small and intermediate values of the cosmological constant. On the other hand, for large cosmological constant, the exponential decay is not followed anymore and there are even some moments that slightly increase. Interestingly, at the final time of the evolutions shown here, different moments $G^{i,j}$ with the same index i approach a common value. From largest to smallest values at the accumulation time the presented moments are: $G^{10,0}$ alone; $G^{8,2}$ with $G^{8,0}$; $G^{6,4}$ with $G^{6,2}$ and $G^{6,0}$; $G^{4,2}$ with $G^{4,0}$; and finally $G^{2,0}$ on its own. The tendency to this behavior can already be noted in the second plot, whereas in the first one all moments gather at a value near 1.
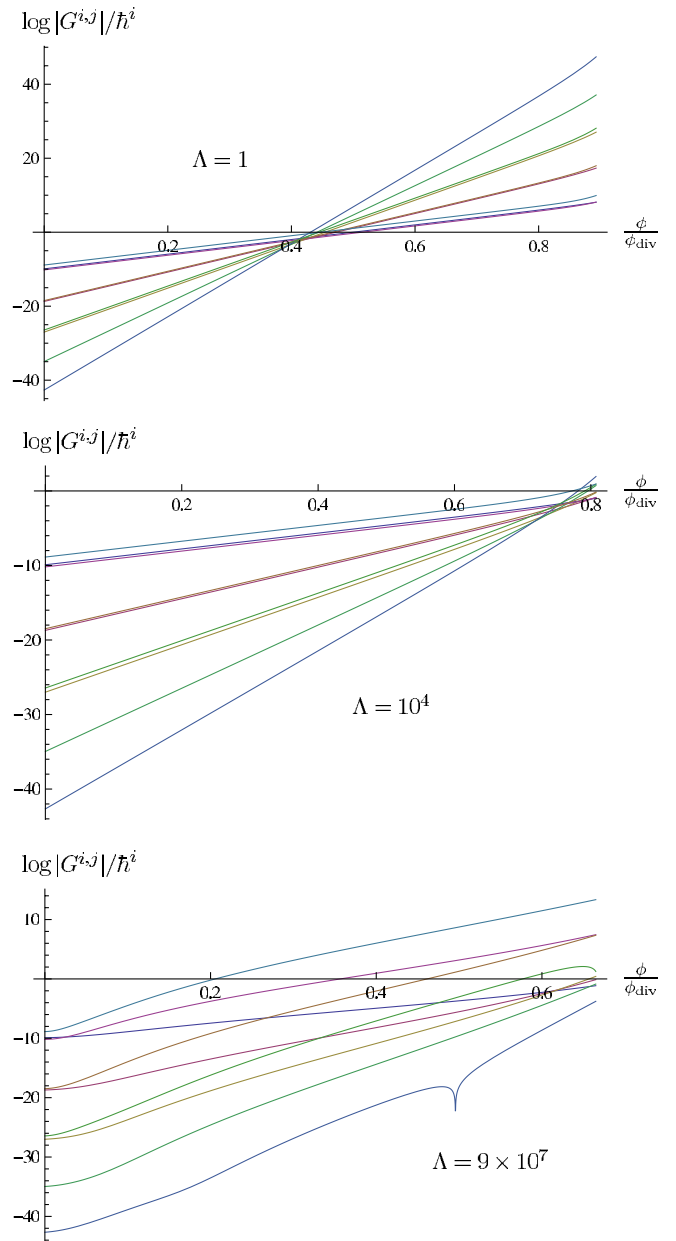
FIG. 7 (color online). This figure corresponds to $G^{i,j}$ with $i < j$ and both i and j even numbers. The value of the cosmological constant is again $\Lambda = 1$, 10^4 and 9×10^7 for different plots. As in the previous case, in the first two plots all moments coincide at a value near 1 at a given time, whereas in the last plot the different variables tend to gather in small sets given by those moments with the same number of $\hat{P}$. In this last plot, at a final time and from largest to smallest value: $G^{4,6}$, then the three $G^{2,i}$, and finally the five $G^{0,i}$. Spikes in this and the following plots arise from transitions of the moments through zero, shown in logarithmic form.

about the high-order system of quantum back-reaction. With the numerical results, we can now provide additional indications regarding quantum evolution, but also new properties become visible.
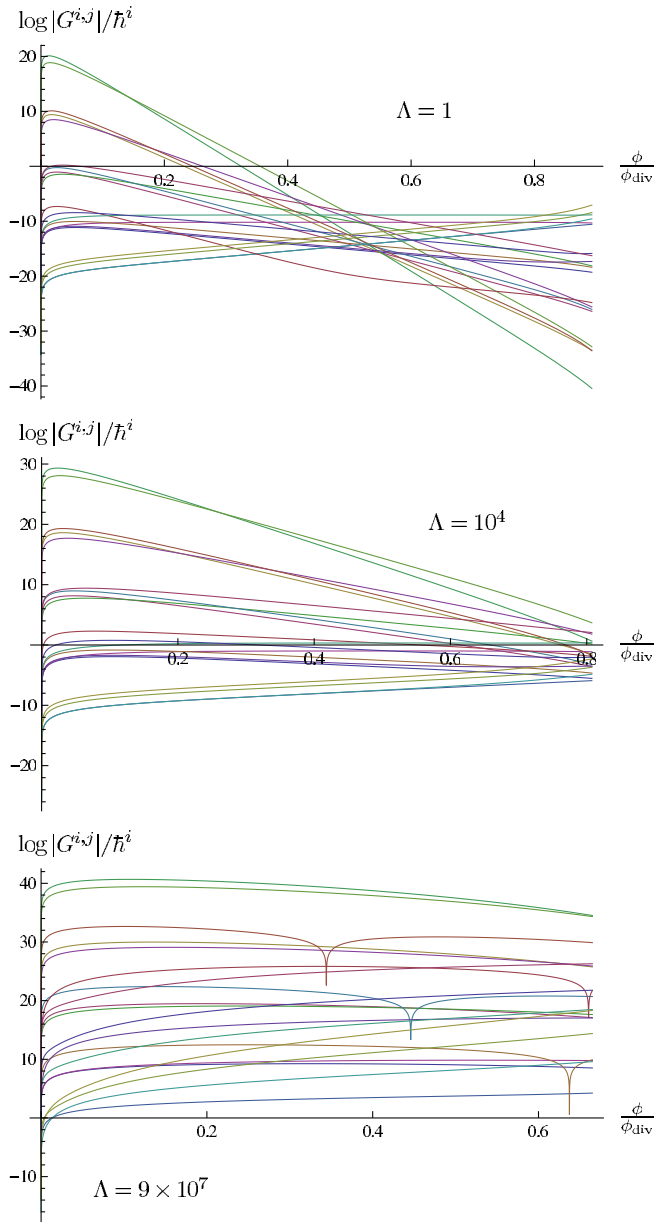
FIG. 8 (color online). This figure corresponds to initially vanishing $G^{i,j}$ with $i > j$. The same values of Λ as in previous cases for each plot apply. Since the initial state we have picked is not adapted to the equations of motion, at the initial time all these modes are excited. Their absolute value after this excitation is approximately ordered by increasing $(i - j)$. That is, the largest moment is $G^{9,0}$, then $G^{9,1}$, $G^{8,1}$, ... On the other hand, it is also interesting to note that this excitation becomes larger with an increasing Λ. Finally, in the case with vanishing Λ, all these moments are exponentially decreasing. This behavior is qualitatively disappearing as one considers a larger cosmological constant.

FIG. 9 (color online). This figure shows the initially vanishing moments $G^{i,j}$ with $i \leq j$. The same values of Λ as in previous cases for each plot apply. As in the previous case, initially all moments are excited to a given value, which is larger with an increasing $(i - j)$. In this way, the moments with lowest absolute value are $G^{0,9}$, $G^{1,9}$, $G^{1,8}$, ... On the other hand, and contrary to the previous case, the qualitative behavior of these moments is kept the same as in the case with $\Lambda = 0$ even for large values of the cosmological constant.

First, the strong increase of some of the moments already seen at second order is confirmed. The system is thus necessarily one of strong quantum back-reaction. Resul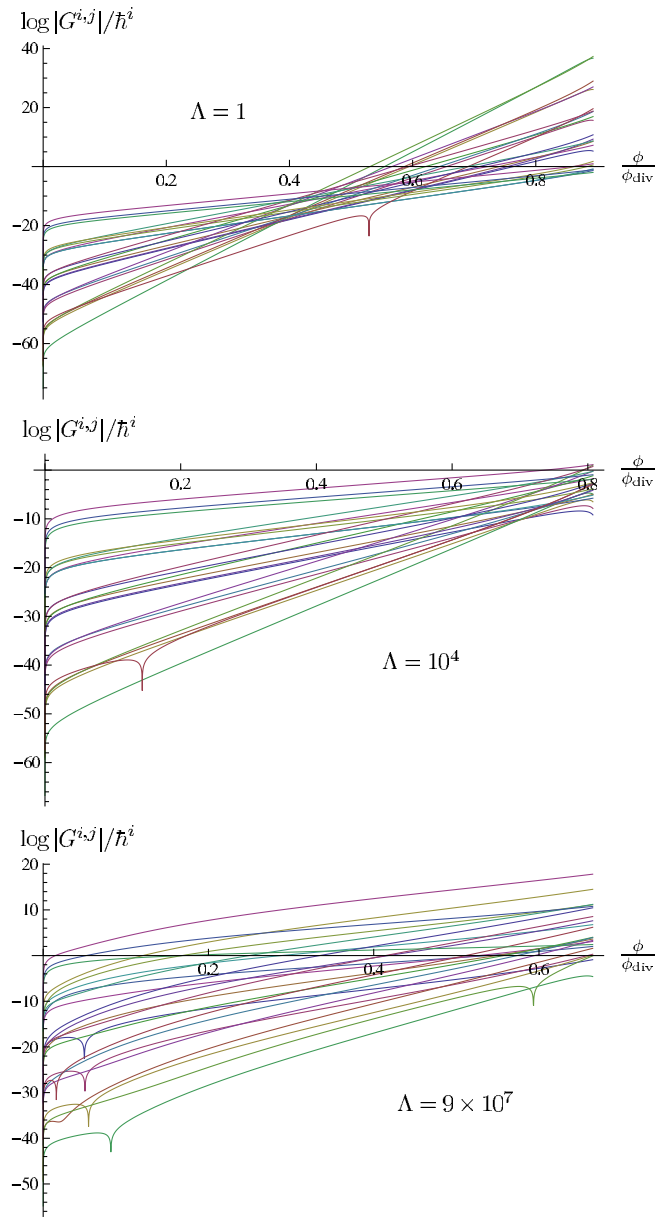ts about self-adjoint extensions of quantum Hamiltonians have suggested that the evolution can be continued through the classical divergence of the volume. The only intuitive semiclassical interpretation would be that quantum corrections become so strong that they can trigger a recollapse. Our numerical results to the orders specified do not provide any indication for this; they rather show that the divergence is enhanced by quantum corrections.

The behavior of the moments confirms two expectations about state evolution. First, several moments grow and become dominant providing strong quantum back-reaction. Secondly, the state rapidly departs from the initially chosen Gaussian moments. While it is difficult to reconstruct a wave function from the moments, it is clear from several of their properties that the state cannot remain Gaussian. A Gaussian state has vanishing moments of odd order, a property which is immediately violated once the state is evolved. As the rapid initial increase of the odd-order moments shown in Figs. 8 and 9 shows, the evolution quickly adapts the state to one whose moments change less severely. To some degree, even the special choice of a Gaussian state may not be much of a restriction since the evolution soon leads to a more suitable dynamical state. However, for robust conclusions about quantum evolution from a fixed set of initial values one must analyze how the state settled down to depends on the initial moments. If different sets of initial moments still lead to adapted states, but ones that differ from the Gaussian adapted state in a way sensitive to the initial set, the quantum behavior would be hard to predict without knowledge of what state may be preferred. Here, much more numerical analysis of the large parameter space involved is necessary.

Finally, we see from figures such as Figs. 8 and 9 that a hierarchy of the moments is maintained for a rather long time even throughout the phase of dynamically adapting the state. Moments of different orders clearly fall into distinct classes as for their behavior of decay or increase. Only when moments of different orders converge, which interestingly happens in a very narrow time frame for all orders shown, will the hierarchy be broken. At such a point, the state can no longer be considered semiclassical, and truncations of the infinite system of effective equations (and the asymptotic expansion they represent) become more difficult to justify in general terms. Nevertheless, in our specific case, even when the state is no longer of recognizably semiclassical form, the truncation is still justified by the convergence analysis we perform in Appendix A. We have also shown the evolution even after that time of accumulation because it indicates another feature. After the accumulation, the moments again separate into clearly demarcated sets, indicating that another hierarchy arises. However, since one has to evolve through an anhierarchical point, it is not clear whether this feature is one of the full system or an artifact of the truncation. Finally and somewhat unexpectedly, the hierarchy is maintained longer for larger values of the cosmological constant, even though the deviation from the harmonic model is then stronger.

V. DISCUSSION

The main contribution of this article is the introduction of a new computational method to analyze quantum back-reaction of quantum mechanical or quantum cosmological systems. We have shown that the use of efficient computer-algebra tools in combination with the closed formula for the Poisson brackets of two generic moments has been essential to push the feasibility of computations to very high order. In particular, the example we have studied of a spatially flat, isotropic universe with a positive cosmological constant and a free, massless scalar field already indicates the usefulness of these methods.

Our analysis has found several new properties of state evolution, some of which were quite unexpected. For example, the state rapidly deviates from the initial Gaussian form (in the volume), but then settles down to another shape obeying a hierarchy of the moments. In this range, truncations used to analyze effective equations remain justified. At some point, the moments converge, interestingly at about the same time. Several properties found here remain without an analytical explanation, stimulating further studies. For instance, somewhat counterintuitively, the moments happen to ''slow down'' their evolution as the value of the cosmological constant increases. That is, qualitatively they follow the same pattern, independently of Λ, but everything happens later for large values of the cosmological constant. Another interesting feature comes from the evolution of the initially nonvanishing moments $G^{i,j}$: at late times they accumulate at a common value for each index i.

On the other hand, we have also studied the convergence of this truncated system of equations with respect to the order (see Appendix A) by analyzing the relative error in the trajectory of the expectation value of the volume V. Remarkably, even though *a priori* we expect only asymptotic rather than convergent expansions, the results converge exponentially for all considered times within a large range of orders. This means that our results reliably reproduce the full quantum behavior of the system even quite near the divergence.

Finally, details of the numerics remain to be explored, most importantly those related to the large parameter space involved. For instance, it is not clear yet how strong the role of the choice of an initial state is. The shape of the state changes rapidly in a very brief initial phase, as shown by a large change in the moments, and then settles down to a form better conserved by the dynamics. This evolved state seems adapted to the dynamics, but it is not known at present whether differently chosen initial states will give rise to the same kind of dynamically evolving state, nor is it known whether the initial choice could influence the dynamics strongly. For such questions, the parametrization by moments, rather than wave functions, is important because it gives full access to the state space. For instance, one could use a random number generator to construct the initial moments just by restricting to those sets that obey the Schwartz inequalities. This will provide a systematic control to map the whole state space, which would not be achievable by specifying explicit wave functions.

(Of course, one could randomize the coefficients of wave functions in some basis, but the observable meaning of those variations would be much less clear than changes of moments.) Probing the large parameter space of the initial state is the main problem in this context which will benefit from further numerical support. The results of this paper thus show that quantum cosmology provides its own set of problems which are interesting from a numerical perspective, whose solution will then give feedback for the specific form of the dynamics realized.

ACKNOWLEDGMENTS

APPENDIX A: CONVERGENCE OF THE SYSTEM WITH AN INCREASING NUMBER OF MOMENTS

In this appendix we address the issue of the convergence of the solution when considering an increasing number of moments. As we have explained in the main body of the article, the existence of a hierarchy on the moments define a semiclassical regime where the truncation of the system into a finite number of moments makes sense. But, since we have obtained the numerical solution of the system of equations at different orders, another method is at our hand to check whether the ignored moments are indeed negligible, namely, to analyze if the difference between the expectation values at different order decreases sufficiently fast.

In order to do so, we define the relative error at order n as,

$$\Delta V_n := 1 - \frac{V_n}{V_{n+1}}, \qquad (A1)$$

where V_n is the expectation value at order n. If this object is convergent sufficiently fast with n, it gives an estimate of the total relative error $(1 - V_n/V_\infty)$ committed when truncating the system at a given order n.

Even though we did not write it explicitly, the object ΔV_n is time (ϕ) dependent and, in fact, we expect it to increase (and eventually not to converge) as we approach the regime of large moments. Hence we have chosen three different times to perform the convergence tests: $0.4\phi_{\text{fin}}$, $0.6\phi_{\text{fin}}$, and $0.9\phi_{\text{fin}}$, where ϕ_{fin} is the final time of each
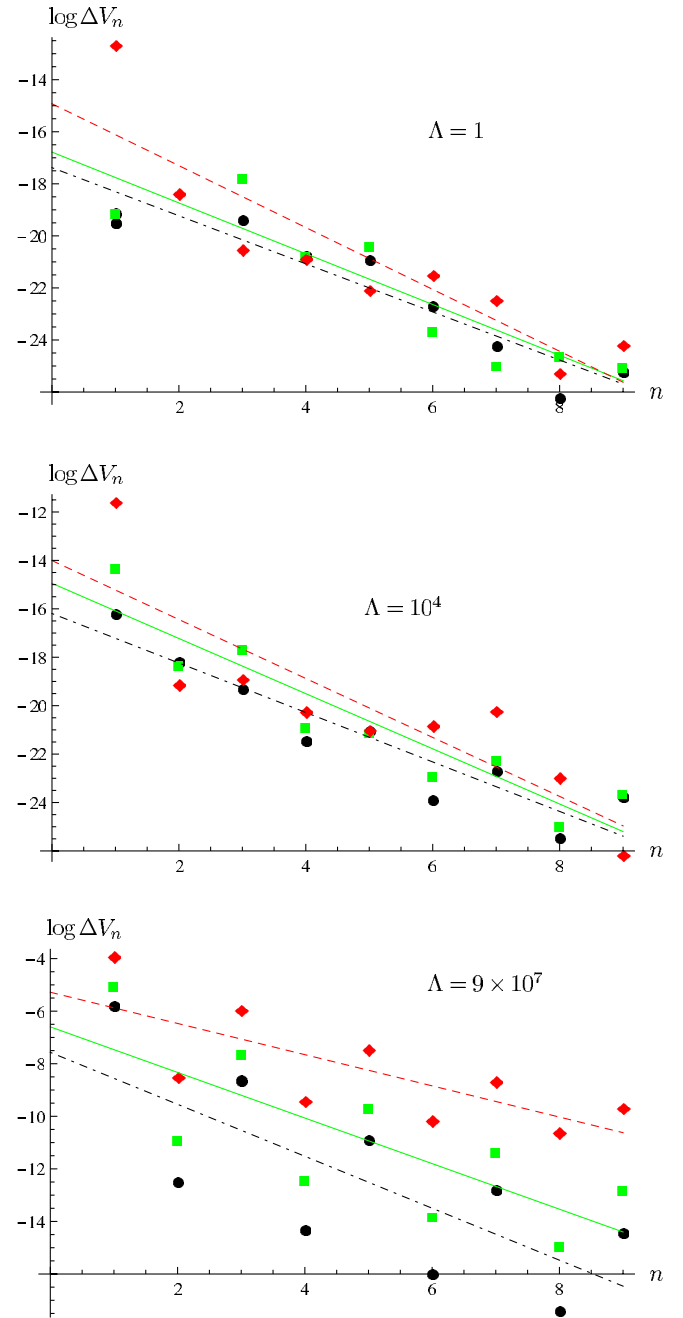

FIG. 10 (color online). In these plots we show the relative change of the volume ΔV_n at each perturbative order for the three different values of the cosmological constant in a logarithmic scale. The computed results and their linear regressions at times $\phi = 0.4\phi_{\text{fin}}$, $\phi = 0.6\phi_{\text{fin}}$, and $\phi = 0.9\phi_{\text{fin}}$ are plotted, respectively, in black (dots and dot-dashed line), green (squares and continuous line) and red (diamonds and dashed line). In the first plot the points at $n = 2$ corresponding to $\phi = 0.4\phi_{\text{fin}}$ and $\phi = 0.6\phi_{\text{fin}}$ are missing because they are exactly (up to our numerical error) zero. These two points have not been considered to perform the corresponding linear regression. The slope of each linear regression gives the convergence order. The absolute value of the different slopes are, from upper to the lower plot and line: 1.22, 1.14, 1.02; 1.19, 0.98, 0.92; and 0.59, 0.87, 0.99.

numerical evolution and takes the value $0.893\phi_{\mathrm{div}}$ for $\Lambda = 1$, $0.807\phi_{\mathrm{div}}$ for $\Lambda = 10^4$, and $0.665\phi_{\mathrm{div}}$ for $\Lambda = 9 \times 10^7$.

These convergence tests are shown in Fig. 10 in a natural logarithmic scale. Firstly, we note that the convergence is exponential in all the cases and for all considered times. Therefore, we have performed linear regressions for all the data.

As expected, the magnitude of the errors increases for later times in all cases. Even so, surprisingly for the first two plots, the convergence is faster at those times. The numerical value of the errors is also increasing with the value of Λ. For instance, the relative errors of the classical solutions ($n = 1$) are of the order $e^{-6} - e^{-4} \approx 10^{-3}$–$10^{-2}$ for large $\Lambda = 9 \times 10^7$, whereas for small $\Lambda = 1$ they are only of order $e^{-16} - e^{-11} \approx 10^{-7}$–$10^{-5}$. This gives an idea of the magnitude of the back-reaction in each case.

On the other hand, we see that our result at 10th order mimics very accurately the behavior of the whole quantum system, in the sense of an asymptotic expansion. In particular, the largest error we find corresponds to the large cosmological constant case at late times ($0.9\phi_{\mathrm{fin}}$) and it is of the order of $e^{-9} \approx 10^{-4}$.

Note that in the last plot of Fig. 10 (and also in the second one, but less severe so) even and odd orders show different convergence behaviors. This observation demonstrates that moments of odd orders continue to contribute less significantly to the volume expectation value than moments of even order, even after the state has evolved away from Gaussian form for which odd-order moments vanish. [For odd n, the expectation values in the ratio
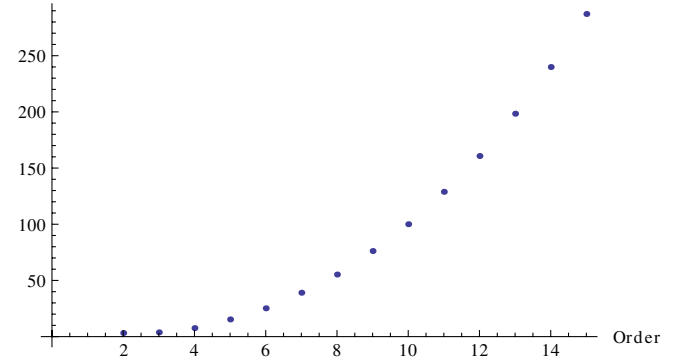

FIG. 11 (color online). In this plot we show the average number of terms that appear in each evolution equation with respect to the order. The dependence is exponential.

V_n/V_{n+1} in (A1) differ by even-order moments, and the errors are seen to be enlarged in the plots.]

This analysis proves that our treatment provides a valid approximation at all considered times, a result which strengthens the motivation to study this general approach.

APPENDIX B: HIGH-ORDER EQUATIONS

In order to give a flavor of the increase in complexity of the equations at high orders, in Fig. 11 we show the average number of terms per equation at each order. In addition, in this appendix, we also present explicitly the complete fifth-order equations of motion (with $\hbar = 1$).

$$\dot{P} = \frac{3\Lambda G^{2,0}}{4(P^2 - \Lambda)^{3/2}} - \frac{3P\Lambda G^{3,0}}{4(P^2 - \Lambda)^{5/2}} + \frac{3\Lambda(4P^2 + \Lambda)G^{4,0}}{16(P^2 - \Lambda)^{7/2}} - \frac{3P\Lambda(4P^2 + 3\Lambda)G^{5,0}}{16(P^2 - \Lambda)^{9/2}} - \frac{3\sqrt{P^2 - \Lambda}}{2}$$

$$\dot{V} = \frac{9P\Lambda G^{2,0}V}{4(P^2 - \Lambda)^{5/2}} - \frac{3\Lambda(4P^2 + \Lambda)G^{3,0}V}{4(P^2 - \Lambda)^{7/2}} + \frac{15P\Lambda(4P^2 + 3\Lambda)G^{4,0}V}{16(P^2 - \Lambda)^{9/2}} - \frac{9\Lambda(8P^4 + 12\Lambda P^2 + \Lambda^2)G^{5,0}V}{16(P^2 - \Lambda)^{11/2}} + \frac{3PV}{2\sqrt{P^2 - \Lambda}}$$
$$- \frac{3\Lambda G^{1,1}}{2(P^2 - \Lambda)^{3/2}} + \frac{9P\Lambda G^{2,1}}{4(P^2 - \Lambda)^{5/2}} - \frac{3\Lambda(4P^2 + \Lambda)G^{3,1}}{4(P^2 - \Lambda)^{7/2}} + \frac{15P\Lambda(4P^2 + 3\Lambda)G^{4,1}}{16(P^2 - \Lambda)^{9/2}}$$

$$\dot{G}^{0,2} = \frac{3PG^{0,2}}{\sqrt{P^2 - \Lambda}} - \frac{3V\Lambda G^{1,1}}{(P^2 - \Lambda)^{3/2}} - \frac{3\Lambda G^{1,2}}{(P^2 - \Lambda)^{3/2}} + \frac{9PV\Lambda G^{2,1}}{2(P^2 - \Lambda)^{5/2}} + \frac{9P\Lambda G^{2,2}}{2(P^2 - \Lambda)^{5/2}} - \frac{3V\Lambda(4P^2 + \Lambda)G^{3,1}}{2(P^2 - \Lambda)^{7/2}}$$
$$- \frac{3\Lambda(4P^2 + \Lambda)G^{3,2}}{2(P^2 - \Lambda)^{7/2}} + \frac{15PV\Lambda(4P^2 + 3\Lambda)G^{4,1}}{8(P^2 - \Lambda)^{9/2}}$$

$$\dot{G}^{0,3} = -\frac{9VG^{1,2}\Lambda}{2(P^2 - \Lambda)^{3/2}} - \frac{9G^{1,3}\Lambda}{2(P^2 - \Lambda)^{3/2}} - \frac{45PV(4P^2 + 3\Lambda)G^{2,0}\Lambda}{16(P^2 - \Lambda)^{9/2}} + \frac{27PVG^{2,2}\Lambda}{4(P^2 - \Lambda)^{5/2}} + \frac{27PG^{2,3}\Lambda}{4(P^2 - \Lambda)^{5/2}}$$
$$- \frac{9V(4P^2 + \Lambda)G^{3,2}\Lambda}{4(P^2 - \Lambda)^{7/2}} - \frac{9PV\Lambda}{8(P^2 - \Lambda)^{5/2}} + \frac{9PG^{0,3}}{2\sqrt{P^2 - \Lambda}} + \left(\frac{9\Lambda(4P^2 + \Lambda)}{8(P^2 - \Lambda)^{7/2}} + \frac{9\Lambda G^{0,2}}{2(P^2 - \Lambda)^{3/2}}\right)G^{1,1}$$
$$+ G^{0,2}\left(-\frac{27PV\Lambda G^{2,0}}{4(P^2 - \Lambda)^{5/2}} - \frac{27P\Lambda G^{2,1}}{4(P^2 - \Lambda)^{5/2}} + \frac{9V\Lambda(4P^2 + \Lambda)G^{3,0}}{4(P^2 - \Lambda)^{7/2}} + \frac{9\Lambda(4P^2 + \Lambda)G^{3,1}}{4(P^2 - \Lambda)^{7/2}} - \frac{45PV\Lambda(4P^2 + 3\Lambda)G^{4,0}}{16(P^2 - \Lambda)^{9/2}}\right)$$

$$\dot{G}^{0,4} = -\frac{9P\Lambda G^{0,2}}{2(P^2-\Lambda)^{5/2}} + \frac{6PG^{0,4}}{\sqrt{P^2-\Lambda}} + \left(\frac{9V\Lambda(4P^2+\Lambda)}{2(P^2-\Lambda)^{7/2}} + \frac{6\Lambda G^{0,3}}{(P^2-\Lambda)^{3/2}}\right)G^{1,1} + \frac{9\Lambda(4P^2+\Lambda)G^{1,2}}{2(P^2-\Lambda)^{7/2}} - \frac{6V\Lambda G^{1,3}}{(P^2-\Lambda)^{3/2}}$$

$$- \frac{6\Lambda G^{1,4}}{(P^2-\Lambda)^{3/2}} - \frac{45PV\Lambda(4P^2+3\Lambda)G^{2,1}}{4(P^2-\Lambda)^{9/2}} + \frac{9PV\Lambda G^{2,3}}{(P^2-\Lambda)^{5/2}} + G^{0,3}\left(-\frac{9PV\Lambda G^{2,0}}{(P^2-\Lambda)^{5/2}} - \frac{9P\Lambda G^{2,1}}{(P^2-\Lambda)^{5/2}}\right.$$

$$+ \frac{3V\Lambda(4P^2+\Lambda)G^{3,0}}{(P^2-\Lambda)^{7/2}} + \frac{3\Lambda(4P^2+\Lambda)G^{3,1}}{(P^2-\Lambda)^{7/2}} - \left.\frac{15PV\Lambda(4P^2+3\Lambda)G^{4,0}}{4(P^2-\Lambda)^{9/2}}\right)$$

$$\dot{G}^{0,5} = \frac{45PV\Lambda(4P^2+3\Lambda)}{32(P^2-\Lambda)^{9/2}} - \frac{225PV\Lambda G^{2,2}(4P^2+3\Lambda)}{8(P^2-\Lambda)^{9/2}} - \frac{45PV\Lambda G^{0,2}}{4(P^2-\Lambda)^{5/2}} - \frac{45P\Lambda G^{0,3}}{4(P^2-\Lambda)^{5/2}} + \frac{15PG^{0,5}}{2\sqrt{P^2-\Lambda}}$$

$$+ \frac{45V\Lambda(4P^2+\Lambda)G^{1,2}}{4(P^2-\Lambda)^{7/2}} + \frac{45\Lambda(4P^2+\Lambda)G^{1,3}}{4(P^2-\Lambda)^{7/2}} - \frac{15V\Lambda G^{1,4}}{2(P^2-\Lambda)^{3/2}} + G^{0,4}\left(\frac{15\Lambda G^{1,1}}{2(P^2-\Lambda)^{3/2}} - \frac{45PV\Lambda G^{2,0}}{4(P^2-\Lambda)^{5/2}}\right.$$

$$- \frac{45P\Lambda G^{2,1}}{4(P^2-\Lambda)^{5/2}} + \frac{15V\Lambda(4P^2+\Lambda)G^{3,0}}{4(P^2-\Lambda)^{7/2}} + \frac{15\Lambda(4P^2+\Lambda)G^{3,1}}{4(P^2-\Lambda)^{7/2}} - \left.\frac{75PV\Lambda(4P^2+3\Lambda)G^{4,0}}{16(P^2-\Lambda)^{9/2}}\right)$$

$$\dot{G}^{1,1} = -\frac{3V\Lambda G^{2,0}}{2(P^2-\Lambda)^{3/2}} - \frac{3\Lambda G^{2,1}}{4(P^2-\Lambda)^{3/2}} + \frac{9PV\Lambda G^{3,0}}{4(P^2-\Lambda)^{5/2}} + \frac{3P\Lambda G^{3,1}}{2(P^2-\Lambda)^{5/2}} - \frac{3V\Lambda(4P^2+\Lambda)G^{4,0}}{4(P^2-\Lambda)^{7/2}}$$

$$- \frac{9\Lambda(4P^2+\Lambda)G^{4,1}}{16(P^2-\Lambda)^{7/2}} + \frac{15PV\Lambda(4P^2+3\Lambda)G^{5,0}}{16(P^2-\Lambda)^{9/2}}$$

$$\dot{G}^{1,2} = \frac{3\Lambda(G^{1,1})^2}{(P^2-\Lambda)^{3/2}} + \left(-\frac{9PV\Lambda G^{2,0}}{2(P^2-\Lambda)^{5/2}} - \frac{9P\Lambda G^{2,1}}{2(P^2-\Lambda)^{5/2}} + \frac{3V\Lambda(4P^2+\Lambda)G^{3,0}}{2(P^2-\Lambda)^{7/2}} + \frac{3\Lambda(4P^2+\Lambda)G^{3,1}}{2(P^2-\Lambda)^{7/2}}\right.$$

$$- \left.\frac{15PV\Lambda(4P^2+3\Lambda)G^{4,0}}{8(P^2-\Lambda)^{9/2}}\right)G^{1,1} - \frac{3\Lambda}{8(P^2-\Lambda)^{3/2}} + \frac{3PG^{1,2}}{2\sqrt{P^2-\Lambda}} + \left(-\frac{9\Lambda(4P^2+\Lambda)}{16(P^2-\Lambda)^{7/2}} - \frac{3\Lambda G^{0,2}}{4(P^2-\Lambda)^{3/2}}\right)G^{2,0}$$

$$- \frac{3V\Lambda G^{2,1}}{(P^2-\Lambda)^{3/2}} - \frac{9\Lambda G^{2,2}}{4(P^2-\Lambda)^{3/2}} + \frac{9PV\Lambda G^{3,1}}{2(P^2-\Lambda)^{5/2}} + \frac{15P\Lambda G^{3,2}}{4(P^2-\Lambda)^{5/2}} + G^{0,2}\left(\frac{3P\Lambda G^{3,0}}{4(P^2-\Lambda)^{5/2}} - \frac{3\Lambda(4P^2+\Lambda)G^{4,0}}{16(P^2-\Lambda)^{7/2}}\right)$$

$$- \frac{3V\Lambda(4P^2+\Lambda)G^{4,1}}{2(P^2-\Lambda)^{7/2}}$$

$$\dot{G}^{1,3} = G^{1,1}\left(\frac{9G^{1,2}\Lambda}{2(P^2-\Lambda)^{3/2}} + \frac{9P\Lambda}{4(P^2-\Lambda)^{5/2}}\right) + \frac{3PG^{1,3}}{\sqrt{P^2-\Lambda}} + \left(\frac{9V\Lambda(4P^2+\Lambda)}{8(P^2-\Lambda)^{7/2}} - \frac{3\Lambda G^{0,3}}{4(P^2-\Lambda)^{3/2}}\right)G^{2,0}$$

$$- \frac{9\Lambda(4P^2+\Lambda)G^{2,1}}{16(P^2-\Lambda)^{7/2}} - \frac{9V\Lambda G^{2,2}}{2(P^2-\Lambda)^{3/2}} - \frac{15\Lambda G^{2,3}}{4(P^2-\Lambda)^{3/2}} - \frac{45PV\Lambda(4P^2+3\Lambda)G^{3,0}}{16(P^2-\Lambda)^{9/2}} + \frac{27PV\Lambda G^{3,2}}{4(P^2-\Lambda)^{5/2}}$$

$$+ G^{0,3}\left(\frac{3P\Lambda G^{3,0}}{4(P^2-\Lambda)^{5/2}} - \frac{3\Lambda(4P^2+\Lambda)G^{4,0}}{16(P^2-\Lambda)^{7/2}}\right) + G^{1,2}\left(-\frac{27PV\Lambda G^{2,0}}{4(P^2-\Lambda)^{5/2}} - \frac{27P\Lambda G^{2,1}}{4(P^2-\Lambda)^{5/2}} + \frac{9V\Lambda(4P^2+\Lambda)G^{3,0}}{4(P^2-\Lambda)^{7/2}}\right.$$

$$+ \left.\frac{9\Lambda(4P^2+\Lambda)G^{3,1}}{4(P^2-\Lambda)^{7/2}} - \frac{45PV\Lambda(4P^2+3\Lambda)G^{4,0}}{16(P^2-\Lambda)^{9/2}}\right)$$

$$\dot{G}^{1,4} = \frac{9\Lambda(4P^2+\Lambda)}{32(P^2-\Lambda)^{7/2}} + \frac{9V\Lambda G^{2,1}(4P^2+\Lambda)}{2(P^2-\Lambda)^{7/2}} + \frac{9\Lambda G^{2,2}(4P^2+\Lambda)}{8(P^2-\Lambda)^{7/2}} - \frac{9\Lambda G^{0,2}}{4(P^2-\Lambda)^{3/2}} + \frac{9P\Lambda G^{1,2}}{4(P^2-\Lambda)^{5/2}}$$

$$+ G^{1,1}\left(\frac{6\Lambda G^{1,3}}{(P^2-\Lambda)^{3/2}} - \frac{9PV\Lambda}{2(P^2-\Lambda)^{5/2}}\right) + \frac{9PG^{1,4}}{2\sqrt{P^2-\Lambda}} - \frac{6V\Lambda G^{2,3}}{(P^2-\Lambda)^{3/2}} - \frac{45PV\Lambda(4P^2+3\Lambda)G^{3,1}}{4(P^2-\Lambda)^{9/2}}$$

$$+ G^{0,4}\left(-\frac{3\Lambda G^{2,0}}{4(P^2-\Lambda)^{3/2}} + \frac{3P\Lambda G^{3,0}}{4(P^2-\Lambda)^{5/2}} - \frac{3\Lambda(4P^2+\Lambda)G^{4,0}}{16(P^2-\Lambda)^{7/2}}\right) + G^{1,3}\left(-\frac{9PV\Lambda G^{2,0}}{(P^2-\Lambda)^{5/2}} - \frac{9P\Lambda G^{2,1}}{(P^2-\Lambda)^{5/2}}\right.$$

$$+ \frac{3V\Lambda(4P^2+\Lambda)G^{3,0}}{(P^2-\Lambda)^{7/2}} + \frac{3\Lambda(4P^2+\Lambda)G^{3,1}}{(P^2-\Lambda)^{7/2}} - \left.\frac{15PV\Lambda(4P^2+3\Lambda)G^{4,0}}{4(P^2-\Lambda)^{9/2}}\right)$$

$$\dot{G}^{2,0} = -\frac{3PG^{2,0}}{\sqrt{P^2 - \Lambda}} + \frac{3\Lambda G^{3,0}}{2(P^2 - \Lambda)^{3/2}} - \frac{3P\Lambda G^{4,0}}{2(P^2 - \Lambda)^{5/2}} + \frac{3\Lambda(4P^2 + \Lambda)G^{5,0}}{8(P^2 - \Lambda)^{7/2}}$$

$$\dot{G}^{2,1} = \left(-\frac{9P\Lambda G^{2,1}}{4(P^2 - \Lambda)^{5/2}} + \frac{3V\Lambda(4P^2 + \Lambda)G^{3,0}}{4(P^2 - \Lambda)^{7/2}} + \frac{3\Lambda(4P^2 + \Lambda)G^{3,1}}{4(P^2 - \Lambda)^{7/2}} - \frac{15PV\Lambda(4P^2 + 3\Lambda)G^{4,0}}{16(P^2 - \Lambda)^{9/2}} \right)G^{2,0}$$
$$- \frac{9PV\Lambda(G^{2,0})^2}{4(P^2 - \Lambda)^{5/2}} - \frac{3PG^{2,1}}{2\sqrt{P^2 - \Lambda}} + \left(\frac{3P\Lambda G^{1,1}}{2(P^2 - \Lambda)^{5/2}} - \frac{3V\Lambda}{2(P^2 - \Lambda)^{3/2}} \right)G^{3,0} + \frac{9PV\Lambda G^{4,0}}{4(P^2 - \Lambda)^{5/2}}$$
$$- \frac{3\Lambda(4P^2 + \Lambda)G^{1,1}G^{4,0}}{8(P^2 - \Lambda)^{7/2}} + \frac{3P\Lambda G^{4,1}}{4(P^2 - \Lambda)^{5/2}} - \frac{3V\Lambda(4P^2 + \Lambda)G^{5,0}}{4(P^2 - \Lambda)^{7/2}}$$

$$\dot{G}^{2,2} = -\frac{9P\Lambda(G^{2,1})^2}{2(P^2 - \Lambda)^{5/2}} + \frac{3\Lambda G^{1,1}G^{2,1}}{(P^2 - \Lambda)^{3/2}} + \left(\frac{3V\Lambda(4P^2 + \Lambda)G^{3,0}}{2(P^2 - \Lambda)^{7/2}} + \frac{3\Lambda(4P^2 + \Lambda)G^{3,1}}{2(P^2 - \Lambda)^{7/2}} - \frac{15PV\Lambda(4P^2 + 3\Lambda)G^{4,0}}{8(P^2 - \Lambda)^{9/2}} \right)G^{2,1}$$
$$+ G^{2,0}\left(-\frac{3G^{1,2}\Lambda}{2(P^2 - \Lambda)^{3/2}} - \frac{9PVG^{2,1}\Lambda}{2(P^2 - \Lambda)^{5/2}} + \frac{9P\Lambda}{4(P^2 - \Lambda)^{5/2}} \right) - \frac{9\Lambda(4P^2 + \Lambda)G^{3,0}}{8(P^2 - \Lambda)^{7/2}} - \frac{3V\Lambda G^{3,1}}{(P^2 - \Lambda)^{3/2}} - \frac{3\Lambda G^{3,2}}{2(P^2 - \Lambda)^{3/2}}$$
$$+ G^{1,2}\left(\frac{3P\Lambda G^{3,0}}{2(P^2 - \Lambda)^{5/2}} - \frac{3\Lambda(4P^2 + \Lambda)G^{4,0}}{8(P^2 - \Lambda)^{7/2}} \right) + \frac{9PV\Lambda G^{4,1}}{2(P^2 - \Lambda)^{5/2}}$$

$$\dot{G}^{2,3} = G^{2,1}\left(\frac{45P\Lambda}{8(P^2 - \Lambda)^{5/2}} - \frac{27P\Lambda G^{2,2}}{4(P^2 - \Lambda)^{5/2}} \right) + G^{2,0}\left(-\frac{3G^{1,3}\Lambda}{2(P^2 - \Lambda)^{3/2}} - \frac{27PVG^{2,2}\Lambda}{4(P^2 - \Lambda)^{5/2}} - \frac{9PV\Lambda}{8(P^2 - \Lambda)^{5/2}} \right)$$
$$+ G^{1,1}\left(\frac{9\Lambda G^{2,2}}{2(P^2 - \Lambda)^{3/2}} - \frac{9\Lambda}{4(P^2 - \Lambda)^{3/2}} \right) + \frac{3PG^{2,3}}{2\sqrt{P^2 - \Lambda}} + \frac{9V\Lambda(4P^2 + \Lambda)G^{3,0}}{8(P^2 - \Lambda)^{7/2}} - \frac{9\Lambda(4P^2 + \Lambda)G^{3,1}}{4(P^2 - \Lambda)^{7/2}}$$
$$- \frac{9V\Lambda G^{3,2}}{2(P^2 - \Lambda)^{3/2}} - \frac{45PV\Lambda(4P^2 + 3\Lambda)G^{4,0}}{16(P^2 - \Lambda)^{9/2}} + G^{1,3}\left(\frac{3P\Lambda G^{3,0}}{2(P^2 - \Lambda)^{5/2}} - \frac{3\Lambda(4P^2 + \Lambda)G^{4,0}}{8(P^2 - \Lambda)^{7/2}} \right)$$
$$+ G^{2,2}\left(\frac{9V\Lambda(4P^2 + \Lambda)G^{3,0}}{4(P^2 - \Lambda)^{7/2}} + \frac{9\Lambda(4P^2 + \Lambda)G^{3,1}}{4(P^2 - \Lambda)^{7/2}} - \frac{45PV\Lambda(4P^2 + 3\Lambda)G^{4,0}}{16(P^2 - \Lambda)^{9/2}} \right)$$

$$\dot{G}^{3,0} = -\frac{9\Lambda(G^{2,0})^2}{4(P^2 - \Lambda)^{3/2}} + \left(\frac{9P\Lambda G^{3,0}}{4(P^2 - \Lambda)^{5/2}} - \frac{9\Lambda(4P^2 + \Lambda)G^{4,0}}{16(P^2 - \Lambda)^{7/2}} \right)G^{2,0} - \frac{9PG^{3,0}}{2\sqrt{P^2 - \Lambda}} + \frac{9\Lambda G^{4,0}}{4(P^2 - \Lambda)^{3/2}} - \frac{9P\Lambda G^{5,0}}{4(P^2 - \Lambda)^{5/2}}$$

$$\dot{G}^{3,1} = \frac{3V\Lambda(4P^2 + \Lambda)(G^{3,0})^2}{4(P^2 - \Lambda)^{7/2}} + \frac{3\Lambda G^{1,1}G^{3,0}}{2(P^2 - \Lambda)^{3/2}} + \left(\frac{3\Lambda(4P^2 + \Lambda)G^{3,1}}{4(P^2 - \Lambda)^{7/2}} - \frac{15PV\Lambda(4P^2 + 3\Lambda)G^{4,0}}{16(P^2 - \Lambda)^{9/2}} \right)G^{3,0}$$
$$+ G^{2,0}\left(-\frac{9\Lambda G^{2,1}}{4(P^2 - \Lambda)^{3/2}} - \frac{9PV\Lambda G^{3,0}}{4(P^2 - \Lambda)^{5/2}} \right) - \frac{3PG^{3,1}}{\sqrt{P^2 - \Lambda}} - \frac{3V\Lambda G^{4,0}}{2(P^2 - \Lambda)^{3/2}} - \frac{9\Lambda(4P^2 + \Lambda)G^{2,1}G^{4,0}}{16(P^2 - \Lambda)^{7/2}}$$
$$+ \frac{3\Lambda G^{4,1}}{4(P^2 - \Lambda)^{3/2}} + \frac{9PV\Lambda G^{5,0}}{4(P^2 - \Lambda)^{5/2}}$$

$$\dot{G}^{3,2} = \frac{3\Lambda(4P^2 + \Lambda)(G^{3,1})^2}{2(P^2 - \Lambda)^{7/2}} + \frac{3\Lambda G^{1,1}G^{3,1}}{(P^2 - \Lambda)^{3/2}} + \left(-\frac{9P\Lambda G^{2,1}}{2(P^2 - \Lambda)^{5/2}} - \frac{15PV\Lambda(4P^2 + 3\Lambda)G^{4,0}}{8(P^2 - \Lambda)^{9/2}} \right)G^{3,1}$$
$$+ G^{2,0}\left(-\frac{9G^{2,2}\Lambda}{4(P^2 - \Lambda)^{3/2}} - \frac{9PVG^{3,1}\Lambda}{2(P^2 - \Lambda)^{5/2}} - \frac{9\Lambda}{8(P^2 - \Lambda)^{3/2}} \right) + G^{3,0}\left(\frac{3V(4P^2 + \Lambda)G^{3,1}\Lambda}{2(P^2 - \Lambda)^{7/2}} + \frac{27P\Lambda}{8(P^2 - \Lambda)^{5/2}} \right)$$
$$- \frac{3PG^{3,2}}{2\sqrt{P^2 - \Lambda}} - \frac{27\Lambda(4P^2 + \Lambda)G^{4,0}}{16(P^2 - \Lambda)^{7/2}} + G^{2,2}\left(\frac{9P\Lambda G^{3,0}}{4(P^2 - \Lambda)^{5/2}} - \frac{9\Lambda(4P^2 + \Lambda)G^{4,0}}{16(P^2 - \Lambda)^{7/2}} \right) - \frac{3V\Lambda G^{4,1}}{(P^2 - \Lambda)^{3/2}}$$

$$\dot{G}^{4,0} = \frac{3P\Lambda(G^{3,0})^2}{(P^2 - \Lambda)^{5/2}} - \frac{3\Lambda G^{2,0}G^{3,0}}{(P^2 - \Lambda)^{3/2}} - \frac{3\Lambda(4P^2 + \Lambda)G^{4,0}G^{3,0}}{4(P^2 - \Lambda)^{7/2}} - \frac{6PG^{4,0}}{\sqrt{P^2 - \Lambda}} + \frac{3\Lambda G^{5,0}}{(P^2 - \Lambda)^{3/2}}$$

$$\dot{G}^{4,1} = -\frac{15PV\Lambda(4P^2 + 3\Lambda)(G^{4,0})^2}{16(P^2 - \Lambda)^{9/2}} + \frac{3\Lambda G^{1,1}G^{4,0}}{2(P^2 - \Lambda)^{3/2}} - \frac{9P\Lambda G^{2,1}G^{4,0}}{4(P^2 - \Lambda)^{5/2}} + \frac{3V\Lambda(4P^2 + \Lambda)G^{3,0}G^{4,0}}{4(P^2 - \Lambda)^{7/2}} + \frac{3P\Lambda G^{3,0}G^{3,1}}{(P^2 - \Lambda)^{5/2}}$$

$$+ G^{2,0}\left(-\frac{3\Lambda G^{3,1}}{(P^2 - \Lambda)^{3/2}} - \frac{9PV\Lambda G^{4,0}}{4(P^2 - \Lambda)^{5/2}}\right) - \frac{9PG^{4,1}}{2\sqrt{P^2 - \Lambda}} - \frac{3V\Lambda G^{5,0}}{2(P^2 - \Lambda)^{3/2}}$$

$$\dot{G}^{5,0} = -\frac{15\Lambda(4P^2 + \Lambda)(G^{4,0})^2}{16(P^2 - \Lambda)^{7/2}} - \frac{15\Lambda G^{2,0}G^{4,0}}{4(P^2 - \Lambda)^{3/2}} + \frac{15P\Lambda G^{3,0}G^{4,0}}{4(P^2 - \Lambda)^{5/2}} - \frac{15PG^{5,0}}{2\sqrt{P^2 - \Lambda}}$$

[1] M. Bojowald and A. Skirzewski, Rev. Math. Phys. **18**, 713 (2006).

[2] F. Cametti, G. Jona-Lasinio, C. Presilla, and F. Toninelli, in *Proceedings of the International School of Physics "Enrico Fermi," Course CXLIII*, edited by G. Casati, I. Guarneri, and U. Smilansky (IOS Press, Amsterdam, 2000), p. 431; arXiv:quant-ph/9910065

[3] N. C. Dias, A. Mikovic, and J. N. Prata, J. Math. Phys. (N.Y.) **47**, 082101 (2006).

[4] M. Bojowald, B. Sandhöfer, A. Skirzewski, and A. Tsobanjan, Rev. Math. Phys. **21**, 111 (2009).

[5] J. F. Donoghue, Phys. Rev. Lett. **72**, 2996 (1994).

[6] J. F. Donoghue, Phys. Rev. D **50**, 3874 (1994).

[7] M. Bojowald and A. Tsobanjan, Phys. Rev. D **80**, 125008 (2009).

[8] M. Bojowald and A. Tsobanjan, Classical Quantum Gravity **27**, 145004 (2010).

[9] M. Bojowald, P. A. Höhn, and A. Tsobanjan, Phys. Rev. D **83**, 125023 (2011).

[10] M. Bojowald, P. A. Höhn, and A. Tsobanjan, Classical Quantum Gravity **28**, 035006 (2011).

[11] M. Bojowald, Gen. Relativ. Gravit. **38**, 1771 (2006).

[12] M. Bojowald, Gen. Relativ. Gravit. **40**, 639 (2007).

[13] M. Bojowald and R. Tavakol, Phys. Rev. D **78**, 023515 (2008).

[14] E. Bentivegna and T. Pawlowski, Phys. Rev. D **77**, 124025 (2008).

[15] M. Bojowald, Phys. Rev. D **75**, 081301(R) (2007).

[16] W. Kaminski and J. Lewandowski, Classical Quantum Gravity **25**, 035001 (2008); W. Kaminski and T. Pawlowski, Phys. Rev. D **81**, 024014 (2010).

[17] M. Bojowald, D. Mulryne, W. Nelson, and R. Tavakol, Phys. Rev. D **82**, 124055 (2010).